Texas Gulf Shoreline Change Rates through 2007

Jeffrey G. Paine, Sojan Mathew, and Tiffany Caudle

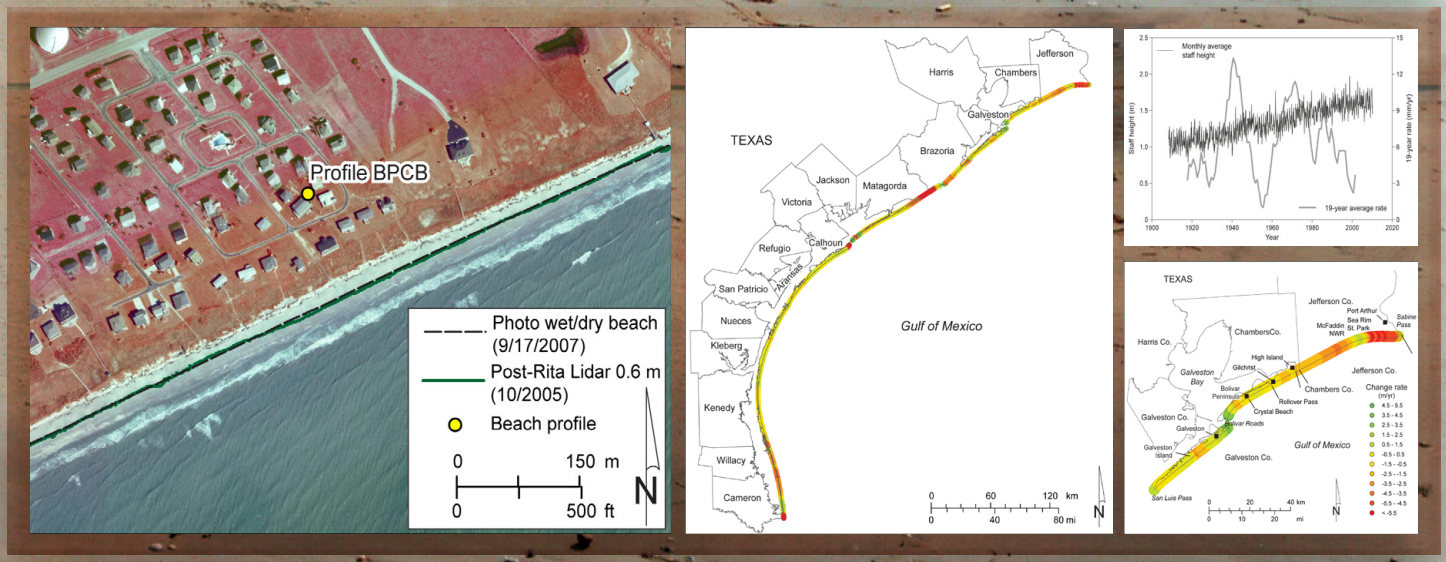

Bureau of Economic Geology
Scott W. Tinker, Director
John A. and Katherine G. Jackson School of Geosciences
The University of Texas at Austin
Austin, Texas 78713-8924

A Report of the Coastal Coordination Council Pursuant to National Oceanic and Atmospheric Administration Award No. NA09NOS4190165

Final Report Prepared for General Land Office under contract no. 10-041-000-3737.

TEXAS GULF SHORELINE CHANGE RATES THROUGH 2007

by

Jeffrey G. Paine, Sojan Mathew, and Tiffany Caudle

Bureau of Economic Geology
John A. and Katherine G. Jackson School of Geosciences
The University of Texas at Austin
University Station, Box X
Austin, Texas 78713

Corresponding author
jeff.paine@beg.utexas.edu
(512) 471-1260
TBPG License No. 3776

A Report of the Coastal Coordination Council Pursuant to National Oceanic and Atmospheric Administration Award No. NA09NOS4190165

Final Report Prepared for the General Land Office under Contract No. 10-041-000-3737.

July 2011

CONTENTS

FIGURES

TABLES

ABSTRACT

Long-term rates of Gulf shoreline change along the Texas coast have been calculated through 2007 from a series of shoreline positions that includes those depicted on 19th century topographic charts (in selected areas), aerial photographs from 1930 to 2007, ground GPS surveys, and airborne Lidar surveys. Net rates of long-term change measured at 11,731 sites spaced at 50 m along the 535 km (332 mi) of Texas shoreline fronting the Gulf of Mexico average 1.24 m/yr of retreat, identical to the average rate of change calculated using linear regression analysis. Net shoreline retreat occurred along 84 percent of the Texas Gulf shoreline, resulting in an estimated net land loss of 5,621 ha (13,890 ac) since 1930 at an average rate of 73 ha/yr (180 ac/yr). Average rates of change are more recessional on the upper Texas coast (-1.6 m/yr east of the Colorado River) than they are on the central and lower coast (-1.0 m/yr from the Colorado River to the Rio Grande).

Notable areas undergoing extensive and significant net shoreline retreat include the muddy marshes on the upper Texas coast between High Island and Sabine Pass, the sandy barrier-island shoreline on Galveston Island west of the seawall, the low, fluvial/deltaic headland constructed by the Brazos and Colorado rivers, the sandy, headland-flanking Matagorda Peninsula west of the Colorado River, San Jose Island (a sandy, central Texas coast barrier island), and the northern end and much of the southern half of Padre Island, a sandy barrier island on the lower Texas coast. Significant net shoreline advance occurred adjacent to the long jetties that protect dredged channels at Sabine Pass, Bolivar Roads, and Aransas Pass, near tidal inlets at the western ends of Galveston Island and Matagorda Peninsula, near the mouth of the Brazos River, along most of Matagorda Island, and on the central part of Padre Island.

Shoreline change rates were calculated for the latest coast-wide aerial photography that predates Hurricane Ike, which struck the upper Texas coast in September 2008 and significantly altered beach and dune morphology and shoreline position. Pre-Ike photography was chosen to avoid emphasizing the nearly instantaneous effects of Ike, recognizing that significant aspects of the recovery process can continue for two or more years after a major storm. The next update of long-term shoreline change rates will be based on shorelines extracted from coast-wide airborne Lidar data scheduled to be acquired in spring 2012.

INTRODUCTION

The Texas coastal zone (fig. 1) is among the most dynamic environments on Earth. Shoreline position is a critical parameter that reflects the balance among several important processes, including sea-level rise, land subsidence, sediment influx, littoral drift, and storm frequency and intensity. Because the Texas coast faces ever-increasing developmental pressures as the coastal population swells, an accurate and frequent analysis of shoreline change serves as a planning tool to identify areas of habitat loss, better quantify threats to residential, industrial, and recreational facilities and transportation infrastructure, and help understand the natural and anthropogenic causes of shoreline change.

The latest trends in shoreline change rates are a critical component in understanding the potential impact that sea level, subsidence, sediment supply, and coastal engineering projects might have on burgeoning coastal population and sensitive coastal environments such as beaches, dunes, and wetlands. Rapidly eroding shorelines threaten coastal habitat and recreational, residential, transportation, and industrial infrastructure and can also significantly increase the vulnerability of coastal communities to tropical storms. Repeated, periodic assessments of shoreline position, rates of change, and factors contributing to shoreline change give citizens, organizations, planners, and regulators an indication of expected future change and help determine whether those changes are accelerating, decelerating, or continuing at the same rate as past changes.

Historical change rates of the Texas Gulf shoreline were first determined by the Bureau of Economic Geology (Bureau) in the 1970s and presented in a series of publications separated at natural boundaries along the 535 km (332 mi) of shoreline (Morton, 1974, 1975, 1977; Morton and Pieper, 1975a, 1975b, 1976, 1977a, 1977b; Morton and others, 1976). This publication series presented net long-term change rates determined from shoreline positions documented on 1850 to 1882 topographic charts published by the U.S. Coast and Geodetic Survey (Shalowitz, 1964) and aerial photographs acquired between about 1930 and 1975. Rates of change for the entire Gulf shoreline were updated through 1982 based on aerial photographs (Paine and Morton, 1989;

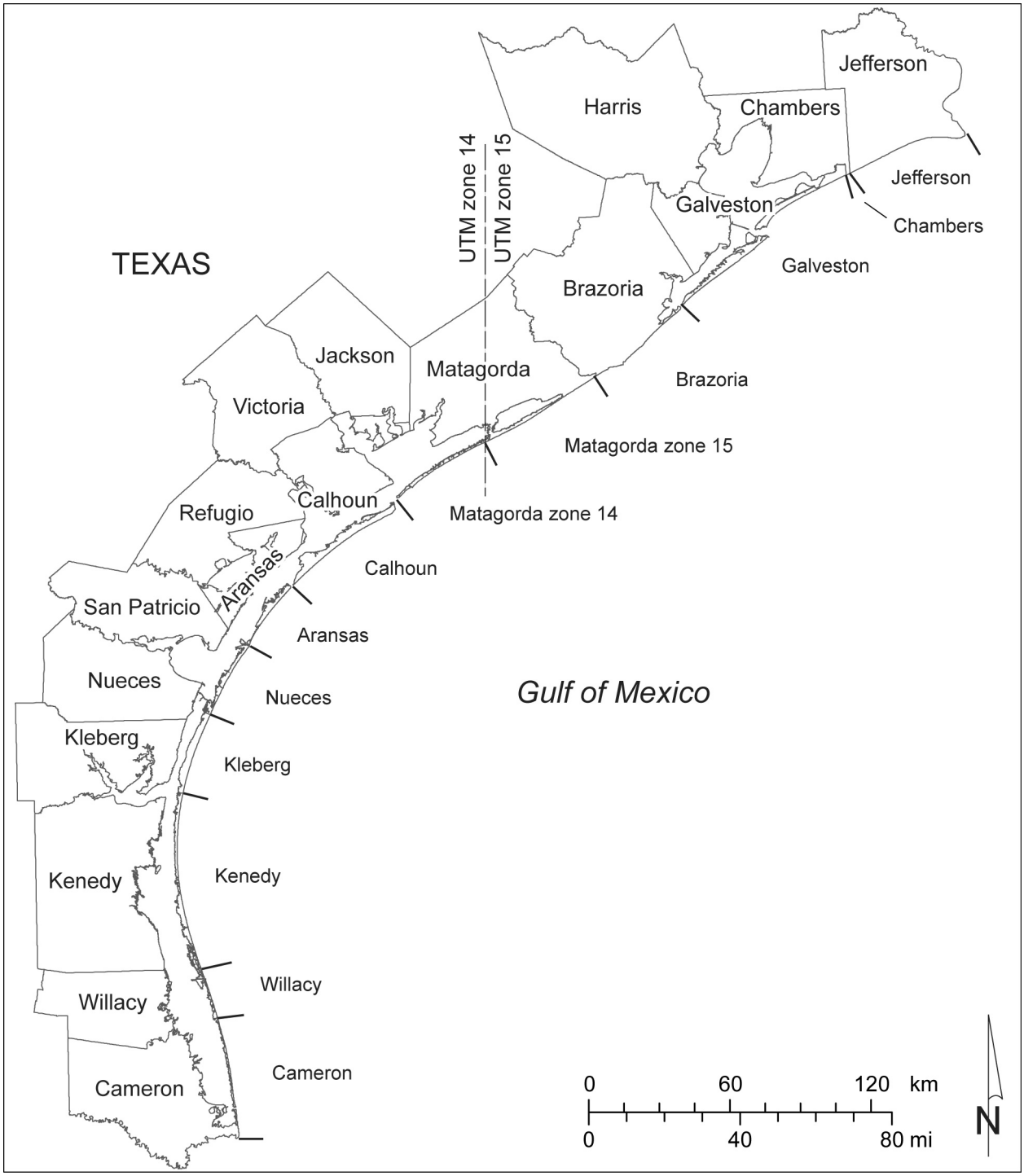

Figure 1. Map of the Texas coastal zone showing counties and the boundary between Universal Transverse Mercator (UTM) zones 14 and 15. Line segments extending seaward from the shoreline mark boundaries between counties with Gulf of Mexico shoreline (Jefferson, Chambers, Galveston, Brazoria, Matagorda, Calhoun, Aransas, Nueces, Kleberg, Kenedy, Willacy, and Cameron). County shoreline change statistics are separated at these boundaries.

Morton and Paine, 1990). More recent updates to shoreline change rates for subsets of the Texas Gulf coast have included the upper coast between Sabine Pass and the Brazos River through 1996 (Morton, 1997), the Brazos River to Pass Cavallo (Gibeaut and others, 2000) and Mustang and north Padre Island (Gibeaut and others, 2001) through 2000 using shoreline positions established using an airborne Lidar topographic mapping system. Lidar-derived shoreline positions in 2000-2001 were also used as part of a Gulf-wide assessment of shoreline change that included the Texas coast (Morton and others, 2004).

This report describes the 2007 update to older long-term change rates that were published in various print formats and online by the Bureau in GIS-compatible format. Those rates were calculated from selected shoreline vintages that began in most areas with the 1930s aerial photographs and included Gulf-shoreline-wide aerial photographs acquired through the mid-1990s, ground-based GPS surveys conducted in select areas during the mid-1990s, and coast-wide airborne Lidar surveys acquired in 2000. For this report, we use the wet beach/dry beach shoreline position as interpreted from georeferenced aerial photographs taken in September and October 2007 along with the earlier shorelines used to calculate the pre-2000 rates to update long-term change rates through 2007. We chose 2007 aerial photographs because they were the latest coast-wide imagery that predated Hurricane Ike, a category 2 hurricane that struck the upper Texas coast in September 2008 and had significant impact on beach morphology and shoreline position. Because the Texas coast undergoes a storm recovery process that can last several years, we anticipate that another update of long-term rates will be needed in 2012 after allowing nearly four years for recovery from Hurricane Ike.

Relative Sea Level

Changes in sea level relative to the ground surface have long been recognized as a major contributor to shoreline change (e.g. Bruun 1954, 1962, 1988; Cooper and Pilkey, 2004). Rising sea level inundates low-relief coastal lands causing shoreline retreat by submergence, and elevates

dynamic coastal processes (currents and waves) that can accelerate shoreline retreat by physical erosion. Changes in relative sea level include both changes in the ocean surface elevation (eustatic sea level) and changes in the elevation of the ground caused by subsidence or uplift. Eustatic sea-level change rates, established by monitoring average sea level at long-record tide gauge stations around the world and more recently using satellite altimetry, vary over a range of about 1 to 4 mm/yr. Gutenberg (1941) calculated a eustatic rate of 1.1 mm/yr from tide gauge data. Estimates based on tide gauge data since then have ranged from 1.0 to 1.7 mm/yr (Gornitz and others, 1982; Barnett, 1983; Gornitz and Lebedeff, 1987; Church and White, 2006), although Emery (1980) supported a higher global average of 3.0 mm/yr that is comparable to more recent satellite-based rates. Attempts to remove postglacial isostatic movement and geographical bias from historical tide gauge records resulted in eustatic estimates as high as 2.4 mm/yr (Peltier and Tushingham, 1989). Recent studies that include satellite altimetry data acquired since 1993 indicate that global rates of sea-level rise average 2.8 mm/yr, or 3.1 mm/yr with postglacial rebound removed (Cazenave and Nerem, 2004). Much of this recent rise is interpreted to arise from thermal expansion of the oceans with a possible contribution from melting of glaciers and polar ice (FitzGerald and others, 2008; Cazenave and Nerem, 2004; Leuliette and Miller, 2009).

In major sedimentary basins such as the northwestern Gulf of Mexico, eustatic sea level rise is exacerbated by subsidence. Published rates of relative sea-level rise measured at tide gauges along the Texas coast are higher than eustatic sea-level rates (Swanson and Thurlow, 1973; Lyles and others, 1988; Penland and Ramsey, 1990; Paine, 1991, 1993), ranging from 3.4 to 6.5 mm/yr during the common 1948 to 1986 period for the Galveston Pier 21, Rockport, and Port Isabel tide gauges. These gauges represent single points along the coast and may not be representative of relative sea-level rise along the entire coast. Geodetic releveling data obtained from the National Geodetic Survey at benchmarks along the Texas coast from Galveston Bay to Harlingen show local variation in subsidence rates that would produce average rates of relative sea-level rise ranging from about 2 to more than 20 mm/yr. Despite the wide range, most of the rates fall within the

range observed for the long-term Texas tide gauges, suggesting that the gauges are representative regional indicators of relative sea-level rise (Paine, 1991, 1993).

The most recent relative sea-level rise rates from selected Texas tide gauges ranges from 1.93 to 6.84 mm/yr (Table 1). These rates were calculated by the National Oceanic and Atmospheric Administration through 2006 from periods of record that begin between 1908 (Galveston Pier 21) and 1963 (Port Mansfield). The highest rates (above 5 mm/yr) are calculated for upper and central Texas coast tide gauges at Galveston (Pier 21 and Pleasure Pier), Sabine Pass, and Rockport. The lowest rate (1.93 mm/yr) is calculated for Port Mansfield, which also has the shortest record. The remaining gauges (Port Isabel, north Padre Island, and Freeport) have rates between 3.48 to 4.35 mm/yr.

Galveston Pier 21 has the longest period of record. Long-term rates of sea-level rise calculated from monthly averages of sea level between April 1908 and April 2011 (fig. 2) are 6.31 mm/yr, similar to the NOAA-calculated rate through 2006. Sea-level rise at this gauge has not been constant; calculations of average rate of change over a rolling 19-year window (centered on the mid-date) show multiyear oscillations in average rate that range from 1.0 to 13.3 mm/yr (fig. 2).

Table 1. Long-term rates of relative sea-level rise at select Texas tide gauges through 2006. Data from National Oceanic and Atmospheric Administration.

Gauge	Beginning year	Period	Rate (mm/yr)	95% confidence interval (mm/yr)
Sabine Pass	1958	49	5.66	1.07
Galveston Pier 21	1908	99	6.39	0.28
Galveston Pleasure Pier	1957	50	6.84	0.81
Freeport	1954	53	4.35	1.12
Rockport	1948	59	5.16	0.67
Port Mansfield	1963	44	1.93	0.97
Padre Island	1958	49	3.48	0.75
Port Isabel	1944	63	3.64	0.44

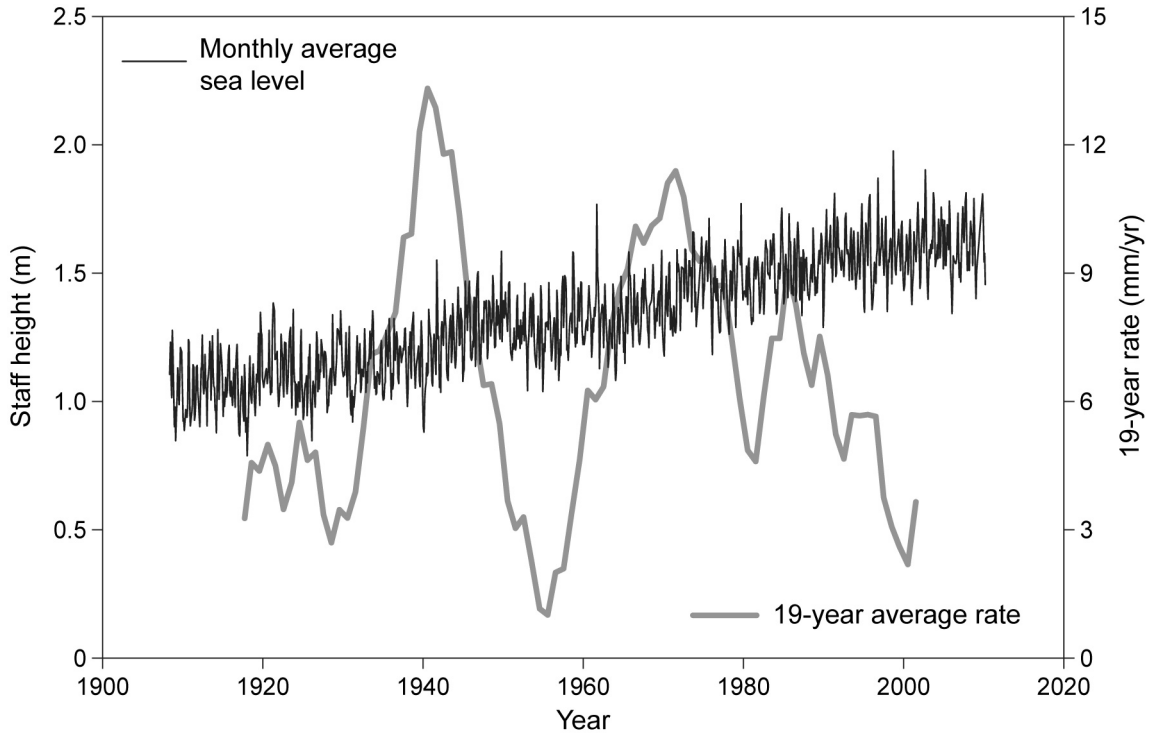

Figure 2. Sea-level trend at Galveston Pleasure Pier, 1908 to 2011. Black line is monthly average sea level. Gray line is the average sea level measured over a 19-year period (the tidal datum epoch) and plotted at the center date of the period. Data from National Oceanic and Atmospheric Administration.

The most recent rates (since about 1990) are 2.1 to 3.7 mm/yr, among the lowest observed at the gauge, and are similar to satellite altimetry-based eustatic rates for the same period.

Tropical Cyclones

There are numerous examples of the significant impact that tropical cyclones (tropical storms and hurricanes) have on the Texas Gulf shoreline (e.g. Price, 1956; Hayes, 1967; Morton and Paine, 1985). These include tropical storms (sustained winds between 62 and 118 km/hr, or 39 and 73 mi/hr) and hurricanes that are classified following the Saffir/Simpson hurricane wind scale (Simpson and Riehl, 1981). Category 1 hurricanes have sustained winds of 119 to 143 km/hr (74 to 95 mi/hr); Category 2: 154 to 177 km/hr (96 to 110 mi/hr); Category 3: 178 to 209 km/hr (111 to 130 mi/hr); Category 4: 210 to 249 km/hr (131 to 155 mi/hr); and Category 5: greater than

249 km/hr (155 mi/hr). In general, minimum central pressures decrease as the categories increase, as does pressure- and wind-driven storm surge. Two critical parameters that influence the erosion potential of a tropical cyclone are surge height and surge duration: generally, the longer sea level is elevated above normal during storm passage, the greater the potential for redistribution of sediment eroded from the beach. Beach and dune recovery after storm passage is a process that includes several distinct stages and can take years (Morton and Paine, 1985; Morton and others, 1994). The ending date (2007) for this update of long-term shoreline change rates was chosen to predate Hurricane Ike (2008), which was a large Category 2 storm that severely eroded the upper Texas coast. We chose not to include post-Ike shorelines to minimize the transient effect of instantaneous erosion and allow for a recovery period before the next shoreline change-rate update.

Historical accounts and records maintained by the National Oceanic and Atmospheric Administration indicate that 64 hurricanes and 56 tropical storms have struck the Texas coast since 1850 (Roth, 2010). On average, there are four hurricanes and four tropical cyclones making landfall in Texas per decade. The longest hurricane-free period in Texas extended nearly 10 years from October 1989 to August 1999 (Roth, 2010). Parts of the Texas coast for which long-term shoreline change rates had not been determined since the early to mid 1990s fall within this hurricane-free period.

From 1993 through 2010, the period most applicable to this study, 17 tropical cyclones have crossed the Texas coast (table 2). This includes 11 tropical storms and 6 hurricanes that ranged in strength from Category 1 to Category 3 at landfall. Only 1 hurricane and 4 tropical storms affected Texas during the 1990s. From 2001 to 2010, that number increased to 5 hurricanes and 7 tropical storms. The most severe were Hurricane Bret, a former Category 4 storm that weakened before landfall on Padre Island in August 1999; Hurricane Rita, a Category 5 storm that weakened to Category 3 before landfall in the Sabine Pass area in September 2005; and Hurricane Ike, once a Category 4 storm that heavily impacted upper Texas coast beaches as a very large

Table 2. Tropical storms affecting the Texas coast between 1990 and 2010. TS = tropical cyclone; H = hurricane; number following H designates numeric strength according to the Saffir/Simpson scale (Simpson and Riehl, 1981). Data from the National Oceanic and Atmospheric Administration and Roth (2010).

Year	Category	Name	Begin date	End date	Landfall area
1993	TS	Arlene	6/18/1993	6/21/1993	North Padre Island
1995	TS	Dean	7/28/1995	8/2/1995	Freeport
1998	TS	Charley	8/21/1998	8/24/1998	Aransas Pass
1998	TS	Frances	9/8/1998	9/13/1998	Matagorda Island
1999	H4	Bret	8/18/1999	8/25/1999	Padre Island (weakened)
2001	TS	Allison	6/5/2001	6/17/2001	Freeport
2002	TS	Bertha	8/4/2002	8/9/2002	North Padre Island
2002	TS	Fay	9/5/2002	9/8/2002	Matagorda Peninsula
2003	H1	Claudette	7/8/2003	7/17/2003	Matagorda Peninsula
2003	TS	Grace	8/30/2003	9/2/2003	Galveston Island
2005	H5	Rita	9/18/2005	9/26/2005	Sabine Pass (H3 at landfall)
2007	TS	Erin	8/15/2007	8/17/2007	San Jose Island
2007	H1	Humberto	9/12/2007	9/14/2007	Upper Texas coast
2008	H2	Dolly	7/20/2008	7/25/2008	South Padre Island
2008	TS	Edouard	8/3/2008	8/6/2008	Upper Texas coast
2008	H4	Ike	9/1/2008	9/15/2008	Galveston (H2 at landfall)
2010	TS	Hermine	9/5/2010	9/9/2010	Rio Grande area

Category 2 storm associated with an unusually high and long-duration storm surge in September 2008. The most recent storm prior to the last shoreline position included in this update is Hurricane Rita, which had the greatest impact on the upper Texas coast. Two years elapsed for beach recovery between that storm and the 2007 update.

Bureau researchers acquired airborne Lidar data on the upper Texas coast after Hurricane Rita in October 2005 and after Hurricane Ike in December 2008. Shorelines extracted from these data have been used to verify shoreline positions mapped on 2007 aerial photographs.

METHODS

Long-term shoreline change rates were calculated by including the 2007 shoreline into the set of shoreline positions that had been used previously to determine long-term Texas Gulf shoreline

change rates presented in the Bureau's shoreline change publication series. Shoreline rates presented in the publications before 2000 were listed as net, or average, rates of change between two end-point dates. More recently, rates have been calculated using linear regression analysis of all included shoreline positions. In the 2007 update, we include both rates. In most cases, these rates are similar and either rate could be used. At measurement sites where the coefficient of determination (goodness of fit) for the calculated linear regression rate is low, net or average rates may be preferred.

Long-term shoreline change rates were calculated following several steps, including:

(1) importing 2007 aerial photographs into a geographic information system data base (ArcGIS, v. 10);

(2) checking the georeferencing of 2007 color aerial photographs against georefenced 2010 aerial photographs acquired by the National Agricultural Inventory Program (NAIP);

(3) mapping the boundary between the wet beach (generally darker tonal colors) and the dry beach (lighter tones) that represents a shoreline proxy that is consistent with that used for older aerial photographs in previous studies and reasonably corresponds with the 1990s boundaries mapped using ground-based GPS receivers (Morton, 1997) and with the 0.6 m mean sea level (msl) elevation contour mapped as the shoreline proxy on digital elevation models produced from the 2000 airborne Lidar surveys (Gibeaut and others, 2000, 2001);

(4) selecting the shoreline vintages to use in the calculation of long-term change rates (table 3), which in most cases includes the earliest photograph-derived shoreline from the 1930's Tobin aerial photographs along with geographically extensive coastal photography from the 1950s, 1960s, 1974, 1990s, and 2007;

(5) creating shore-parallel baselines from which shore-perpendicular transects were cast at 50-m intervals along the shoreline using the GIS-based extension software Digital Shoreline Analysis System (DSAS; Thieler and others, 2009);

(6) calculating long-term rates of change and associated statistics using the transect locations and the selected shorelines within the DSAS extension to ArcGIS; and

(7) determining the intersection of the transect lines with the 2007 shoreline and creating GIS shape files containing the rates, statistics, and period of shoreline change mea-

Table 3. Shoreline dates and types used to calculate Gulf shoreline change rates for each Texas county having shoreline on the open Gulf of Mexico. "T" denotes shorelines depicted on 19th century U.S. Coast and Geodetic Survey charts. "A" denotes shorelines mapped as the wet beach/dry beach boundary on aerial photographs. "G" denotes shorelines mapped using ground-based GPS instruments. "L" denotes shoreline position extracted from airborne Lidar surveys. "p" denotes partial county coverage.

County	Shoreline Dates and Types								
Jefferson	1882 T	1930 A	1955-57 A	1974 A	1982 A	1996 G	2000 L	2007 A	
Chambers	1882 T	1930 A	1957 A	1974 A	1982 A	1996 G	2000 L	2007 A	
Galveston	1838-1852 T,p	1882 T,p	1930-34 A	1956-57 A	1964-65 A	1970 A,p	1996 G	2000 L	2007 A
Brazoria	1930-34 A,p	1956 A	1965 A	1965 A	1974 A	1995 A	2000 L	2007 A	
Matagorda	1930-37 A	1956 A	1965 A	1974 A	1991 A	2000 L	2007 A		
Calhoun	1937 A	1956-57 A	1965 A	1974 A	1995 A	2000 L	2007 A		
Aransas	1931-37 A	1958 A	1965 A	1974 A	1995 A	2000 L	2007 A		
Nueces	1937 A	1958-59 A	1965 A	1974 A	1990 A	1995 A	2000 L	2007 A	
Kleberg	1937-38 A	1956-59 A	1974 A,p	1995 A	2000 L	2007 A			
Kenedy	1937-38 A	1969 A	1974 A	1995 A	2000 L	2007 A			
Willacy	1937 A	1960 A	1975 A	1995 A	2000 L	2007 A			
Cameron	1934-37 A	1960 A	1969 A	1974 A	1991 A,p	1995 A	2000 L	2007 A	

surements and the measurement transects bounded by the most landward and seaward historical shoreline position for each measurement site.

Rates were calculated as linear regression rates and as net (average) rates. Where regression coefficients of determination are relatively high, rates calculated using the linear regression method can be interpreted to reasonably express the long-term movement of the shoreline. Where coefficients are low and fitting errors are high, regression rates may not reasonably reflect the long-term movement of the shoreline. In these cases, net rates that represent the simple average rate of change calculated by dividing the movement distance divided by the elapsed time are preferred.

Shoreline positions on 2007 aerial photographs were mapped by two persons and spot-checked by a third to verify the interpreted position. We also used beach profiles and GPS-mapped shorelines acquired for the Texas High School Coastal Monitoring Program (THSCMP) near the dates of photography to verify the wet beach/dry beach positions at long-term monitoring sites on Galveston Island, Follets Island, Matagorda Peninsula, Mustang Island, and Padre Island (fig. 3). Finally, mapped shoreline positions were compared to shoreline positions extracted from airborne Lidar data acquired on the upper Texas coast in October 2005 after Hurricane Rita.

Sources of Shorelines

As documented in previous Bureau reports, mapped shorelines from the 1800s to 1990 were originally optically transferred to common paper 7.5-minute topographic base maps. The 1996 shoreline (upper coast only) was surveyed using differentially corrected GPS data acquired from a GPS receiver mounted on a motorized vehicle (Morton and others, 1993; Morton, 1997). The 2000 shoreline was surveyed using an Optech ALTM 1225 airborne laser terrain mapping instrument (Lidar). Laser range data were combined with differentially corrected aircraft position determined from GPS and an inertial measurement unit to determine land-surface position and elevation. Shoreline position was extracted from the Lidar-derived digital elevation model at a elevation of 0.6 m above mean sea level (msl). The 2007 shoreline was mapped digitally within a GIS by digitizing the wet beach/dry beach boundary as depicted on high-resolution, georefer-

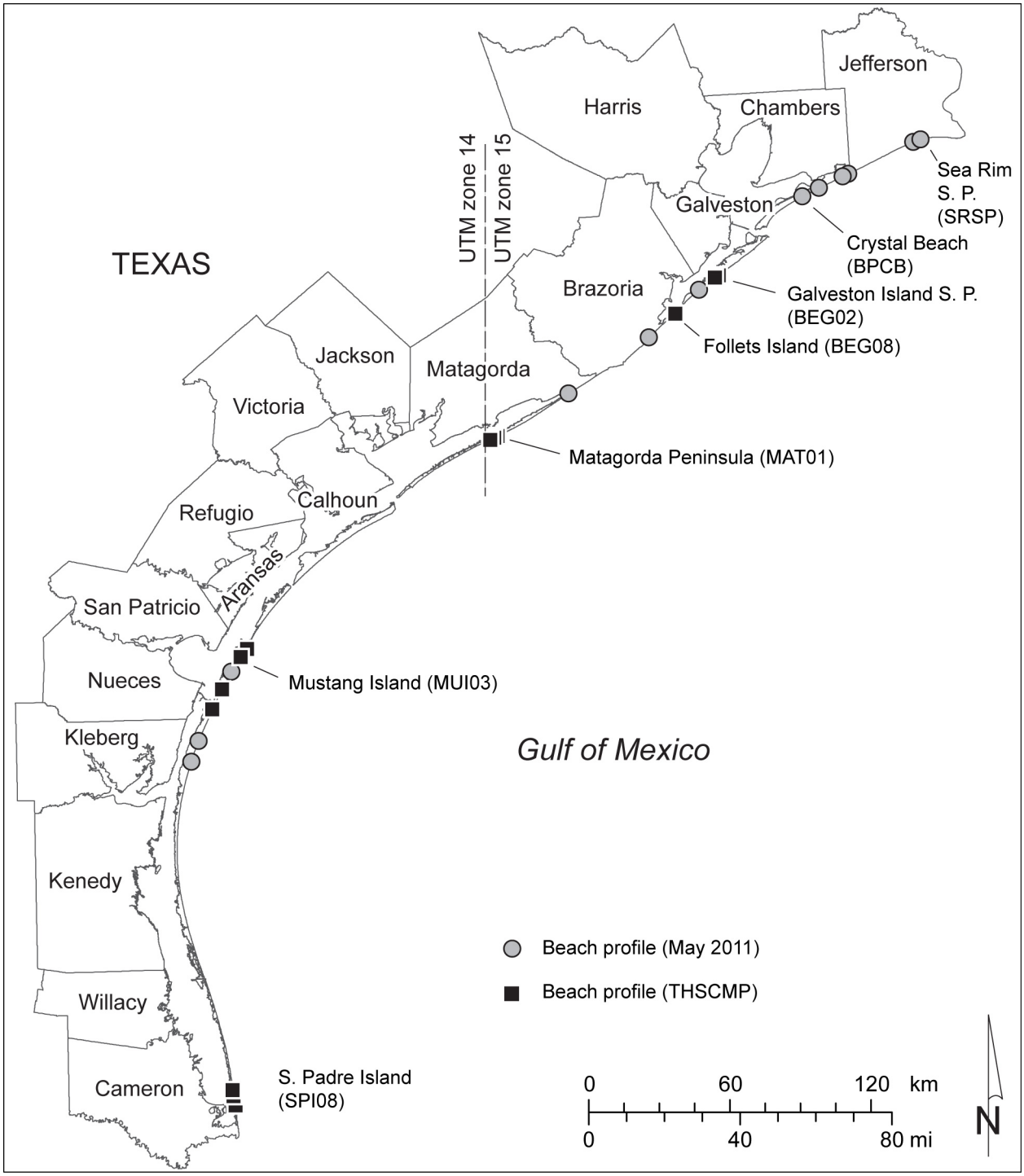

Figure 3. Beach profile and ground GPS survey sites along the Texas Gulf shoreline. Profile sites include those maintained by the Texas High School Coastal Monitoring Program in 2007 and new sites established by the Bureau in 2011.

enced aerial photographs taken in September and October 2007. The position of likely stationary natural features and infrastructure shown on 2007 photographs was compared to the position of correlative features on georeferenced 2010 aerial photographs to ensure accurate positioning.

Shorelines were selected for change-rate analysis to conform with shorelines chosen for earlier calculations of shoreline change rate, to generally exclude older shorelines in some areas where major engineered structures have impacted shoreline change, and to give regular intervals between shorelines along a given transect. The software DSAS (Digital Shoreline Analysis System, version 4.2, Thieler and others, 2009) was installed on ArcGIS 9.3 to facilitate calculation and GIS-based analysis of shoreline change.

Positional Verification

The georeferencing of the 2007 aerial photography is one of the principal sources of potential error in the updated calculations of long-term shoreline change rates (Anders and Byrnes, 1991; Crowell and others, 1991; Moore, 2000). Georeferencing was checked through comparison of equivalent natural and constructed features common to 2007 aerial photographs and georeferenced NAIP photographs taken in 2010.

A second positional check, which addressed the georeferencing of the 2007 photographs and the interpretation of the position of the wet beach/dry beach boundary, superimposed GPS-based beach profiles and wet beach/dry beach boundary data acquired in 2007 by the THSCMP and the photo-interpreted 2007 wet beach/dry beach boundary to be used for change rate calculations. These comparisons, in some cases from ground-based data acquired within a few days of the date of aerial photography, generally showed good agreement (within a few m) between boundaries interpreted from ground-based data and those interpreted from aerial photographs. Where there is a small discrepancy in the position of the wet beach/dry beach boundary, the feature mapped on aerial photographs is likely to be more accurately placed than the feature mapped on the ground.

Comparisons of wet beach/dry beach position were conducted for THSCMP beach profile sites at Galveston Island State Park, Follets Island, Mustang Island, and South Padre Island (fig. 3). At Galveston Island State Park (fig. 4), GPS-based wet beach/dry beach boundary mapped on 9/20/2007 at station BEG02 lies generally a few m landward of the same boundary mapped on a 2007 aerial photograph acquired three days earlier (9/17/2007). Analysis of aerial photographs and the beach profile acquired during the ground visit (fig. 5) suggests that the beach feature mapped using GPS could actually be landward of the wet beach/dry beach boundary, and that the photograph-based position is consistent with other geomorphic features identified in the profile. At Follets Island (fig. 6), the ground-based mapping of the wet beach/dry beach boundary on 9/20/2007 near station BEG08 coincides with the same boundary mapped on an aerial photograph taken three days earlier (9/17/2007). The wet beach/dry beach boundary mapped from aerial photography acquired on 9/21/2007, when superimposed on a beach profile acquired using

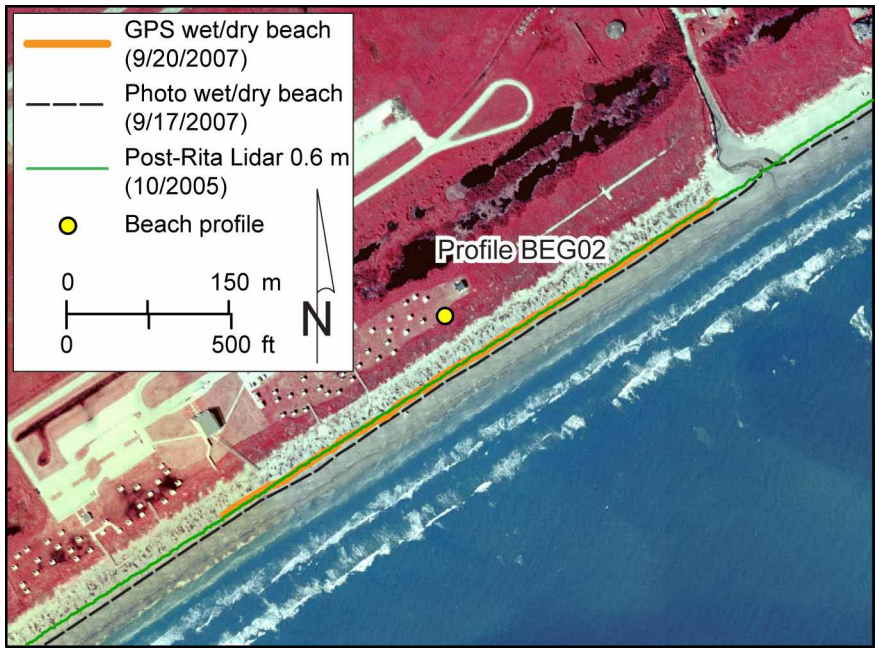

Figure 4. Shoreline position comparison at Galveston Island State Park site BEG02 (fig. 3). Shorelines include the 2007 wet beach/dry beach boundary mapped on aerial photographs taken on 9/17/2007, the wet beach/dry beach boundary mapped on 9/20/2007 by THSCMP students and staff using ground GPS, and the 0.6 m msl shoreline proxy extracted from airborne Lidar data acquired after Hurricane Rita in October 2005.

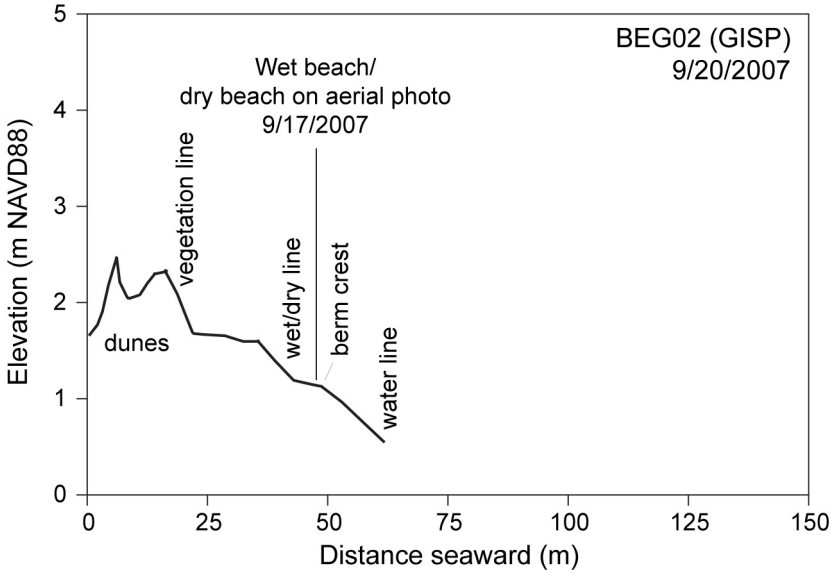

Figure 5. Beach profile at Galveston Island State Park site BEG02 (figs. 3, 4) with superimposed wet beach/dry beach boundary mapped on 2007 aerial photographs. Profile acquired on 9/20/2007 by THSCMP students and staff using ground GPS and Emery rods.

ground-based GPS on Matagorda Peninsula (station MAT01, figs. 3, 7) on 9/28/2007, shows reasonable placement of the wet beach boundary on a gentle slope landward of the berm crest identified on the beach profile. Farther south, GPS-based mapping of the wet beach/dry beach boundary near Mustang Island station MUI03 (figs. 3, 8) on 9/21/2007 shows good agreement with the same boundary mapped on an aerial photograph taken less than a month later (10/17/2007). In addition, the photograph-based boundary lies landward of the berm crest identified in the beach profile, but appropriately well seaward of the dunes and vegetation line (fig. 9). On south Padre Island, a GPS-based beach profile was acquired and the GPS-based wet beach/dry beach boundary was mapped on the narrow beach near station SPI08 on 9/24/2007 (figs. 3, 10). The same feature mapped on an aerial photograph taken on 10/19/2007 generally coincides with the wet/dry line on both the beach profile (fig. 11) and the map, although some real change could have occurred between the dates at this dynamic site.

Finally, we compared 2007 shoreline positions interpreted from aerial photography to shoreline positions extracted at 0.6 m elevation from airborne Lidar surveys of the upper Texas coast acquired as near as possible to the 2007 photography dates. These comparisons were conducted

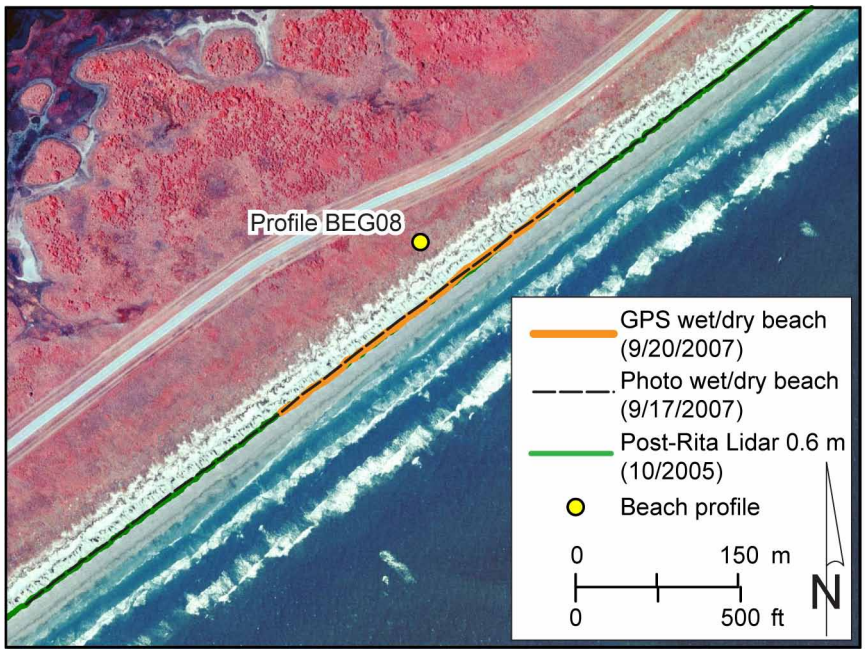

Figure 6. Shoreline position comparison at Follets Island site BEG08 (fig. 3). Shorelines include the 2007 wet beach/dry beach boundary mapped on aerial photographs taken on 9/17/2007, the wet beach/dry beach boundary mapped on 9/20/2007 by THSCMP students and staff using ground GPS, and the 0.6 m msl shoreline proxy extracted from airborne Lidar data acquired after Hurricane Rita in October 2005.

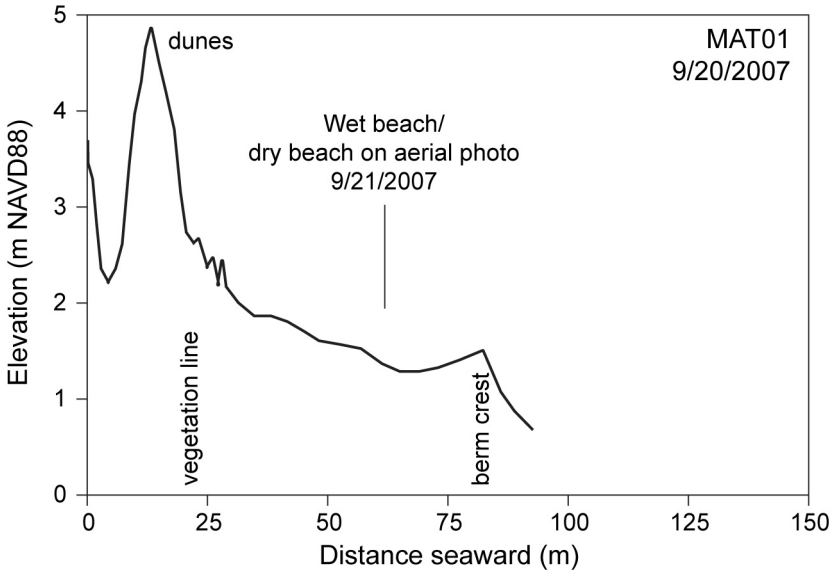

Figure 7. Beach profile at Matagorda Peninsula site MAT01 (fig. 3) with superimposed wet beach/dry beach boundary mapped on 2007 aerial photographs. Profile acquired on 9/20/2007 by THSCMP students and staff using ground GPS and Emery rods.

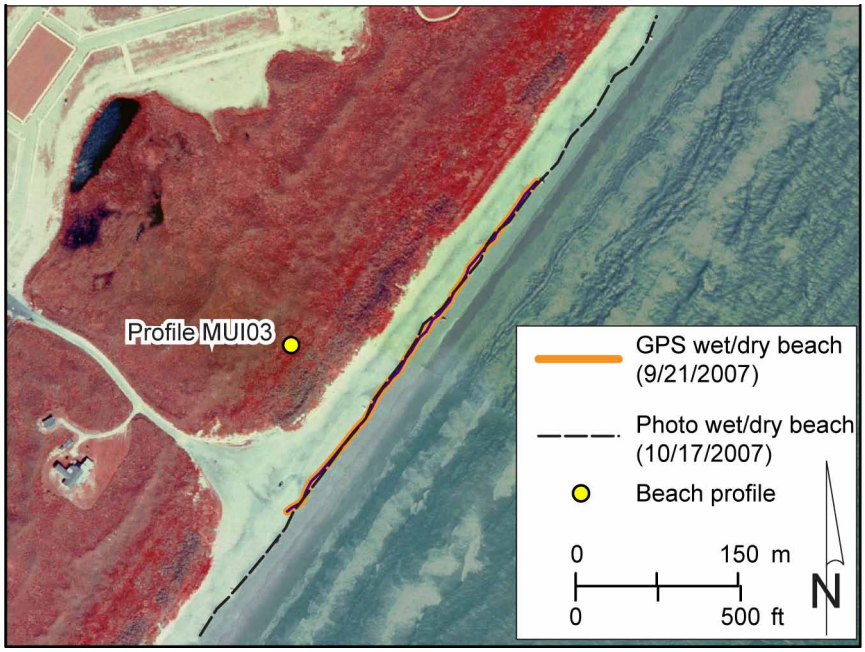

Figure 8. Shoreline position comparison at Mustang Island site MUI03 (fig. 3). Shorelines include the 2007 wet beach/dry beach boundary mapped on aerial photographs taken on 10/17/2007 and the wet beach/dry beach boundary mapped on 9/21/2007 by THSCMP students and staff using ground GPS.

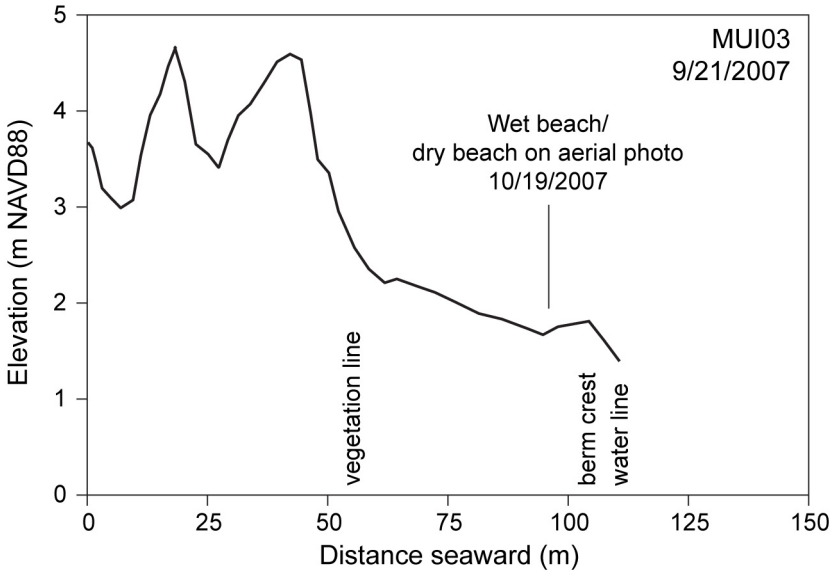

Figure 9. Beach profile at Mustang Island site MUI03 (figs. 3, 8) with superimposed wet beach/ dry beach boundary mapped on 2007 aerial photographs. Profile acquired on 9/21/2007 by THSCMP students and staff using ground GPS and Emery rods.

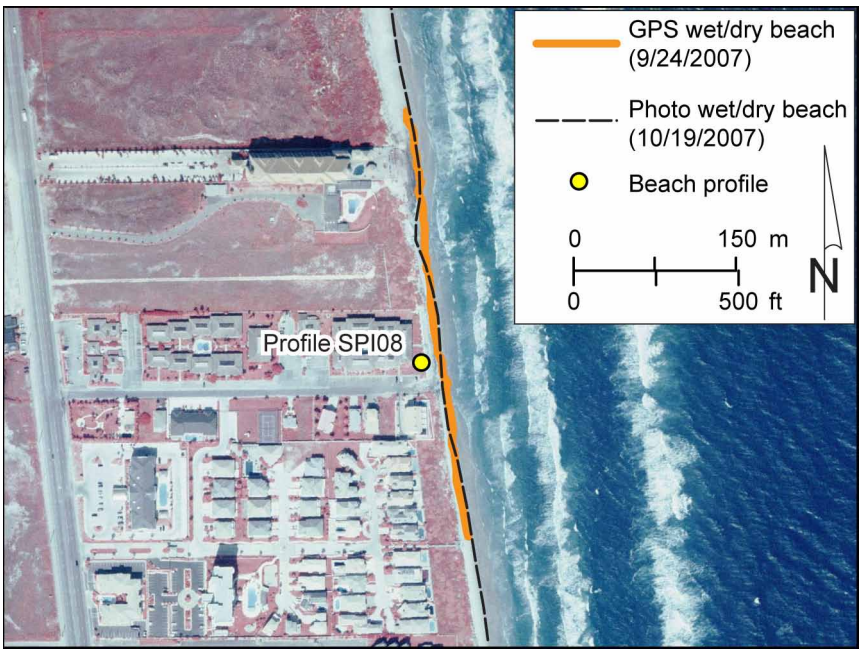

Figure 10. Shoreline position comparison at South Padre Island site SPI08 (fig. 3). Shorelines include the 2007 wet beach/dry beach boundary mapped on aerial photographs taken on 10/19/2007 and the wet beach/dry beach boundary mapped on 9/24/2007 by THSCMP students and staff using ground GPS.

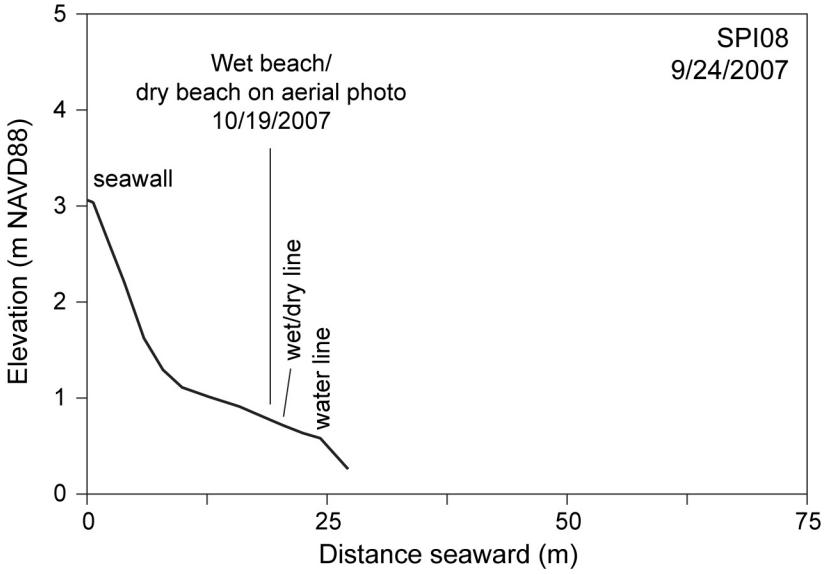

Figure 11. Beach profile at South Padre Island site SPI08 (figs. 3, 10) with superimposed wet beach/dry beach boundary mapped on 2007 aerial photographs. Profile acquired on 9/24/2007 by THSCMP students and staff using ground GPS and Emery rods.

at new beach profile sites at Sea Rim State Park (SRSP, fig. 3) and Crystal Beach on Bolivar Peninsula (BPCB, fig. 3). At Sea Rim State Park, the extracted 0.6 m shoreline determined from airborne Lidar data acquired after Hurricane Rita in October 2005 is generally a few meters landward of the shoreline mapped on aerial photography taken nearly two years later (fig. 12). Because this site was near the landfall area, it is possible that both data sets are correct and the beach advanced an amount equivalent to the relatively minor difference in position during recovery from Rita. At Crystal Beach, the shoreline at 0.6 m elevation extracted from airborne Lidar survey data acquired in October 2005 coincides with the wet beach/dry beach boundary mapped on an aerial photograph acquired on 9/17/2007 (fig. 13), suggesting that there was minor change caused by the passage of Hurricane Rita farther to the east and little subsequent recovery on Bolivar Peninsula. Further comparisons of Lidar-derived beach profiles acquired at the Sea Rim State Park and Crystal Beach profile sites in May 2000 (pre-Rita), October 2005 (post-Rita), and December 2008 (post-Ike) with ground GPS-based profiles acquired in May 2011 (figs. 14, 15) show that (a) the 2007 wet beach/dry beach boundary position is consistent with the post-Rita survey elevation at both sites, (b) Hurricane Ike caused a large loss of beach elevation at Crystal Beach (as much as 2.5 m) and much less vertical change at Sea Rim State Park, and (c) there has been aggradation of the beach of as much as 1 m at Crystal Beach and about 0.5 m at Sea Rim State Park since the passage of Hurricane Ike.

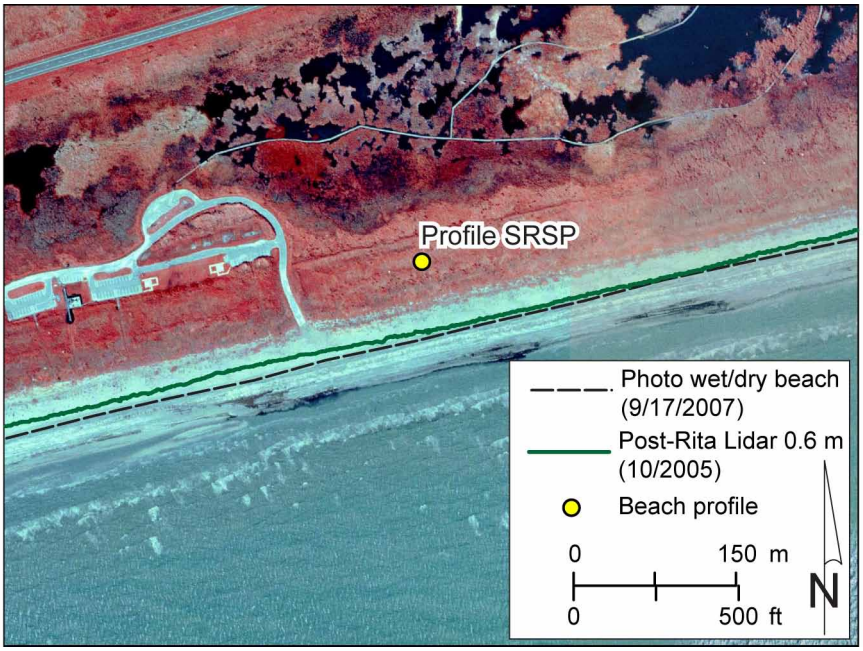

Figure 12. Shoreline position comparison at Sea Rim State Park site SRSP (fig. 3). Shorelines include the 2007 wet beach/dry beach boundary mapped on aerial photographs taken on 9/17/2007 and the 0.6 m msl shoreline proxy extracted from airborne Lidar data acquired after Hurricane Rita in October 2005.

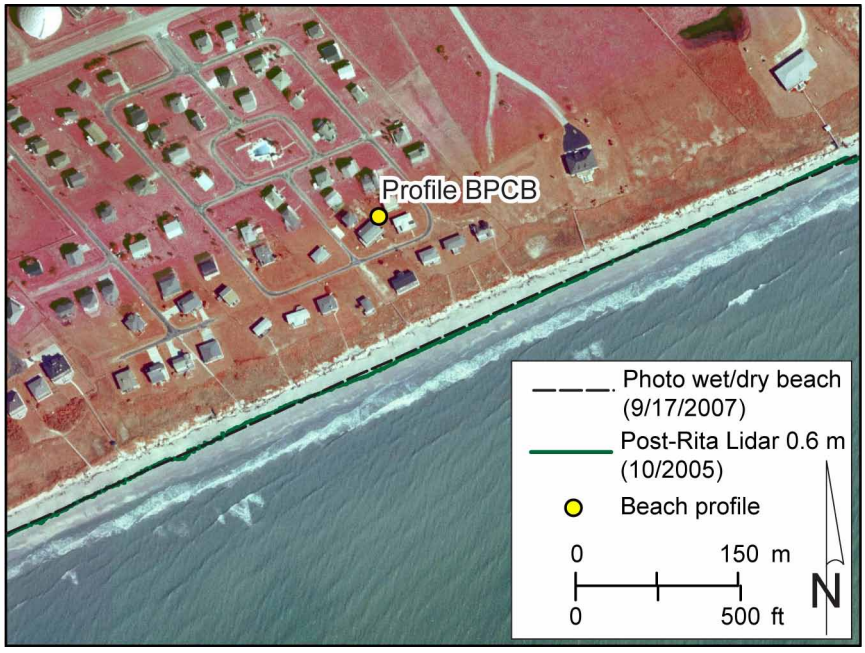

Figure 13. Shoreline position comparison on Bolivar Peninsula at Crystal Beach site BPCB (fig. 3). Shorelines include the 2007 wet beach/dry beach boundary mapped on aerial photographs taken on 9/17/2007 and the 0.6 m msl shoreline proxy extracted from airborne Lidar data acquired after Hurricane Rita in October 2005.

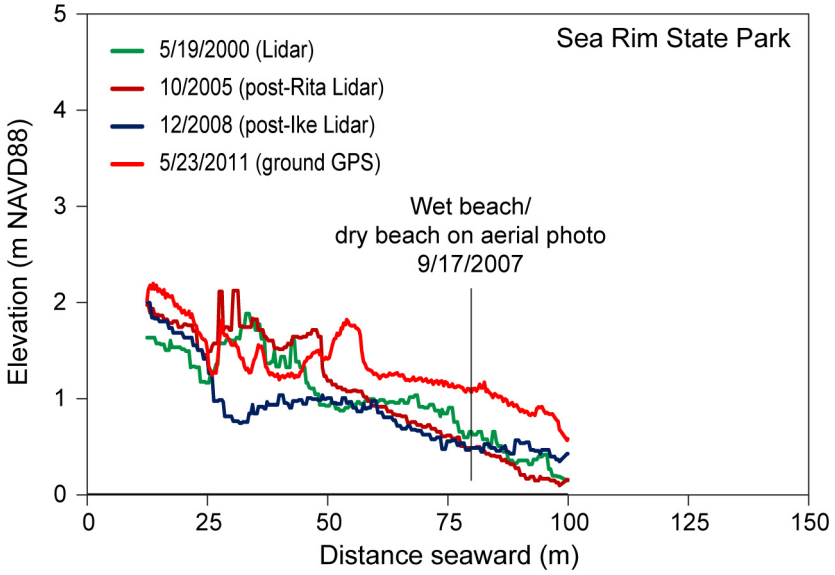

Figure 14. Beach profile at Sea Rim State Park site SRSP (figs. 3, 12) with superimposed wet beach/dry beach boundary mapped on 2007 aerial photographs. Profiles for May 2000, October 2005 (post Rita), and December 2008 (post Ike) were extracted from airborne Lidar surveys. The May 2011 profile was acquired using ground-based differential GPS measurements.

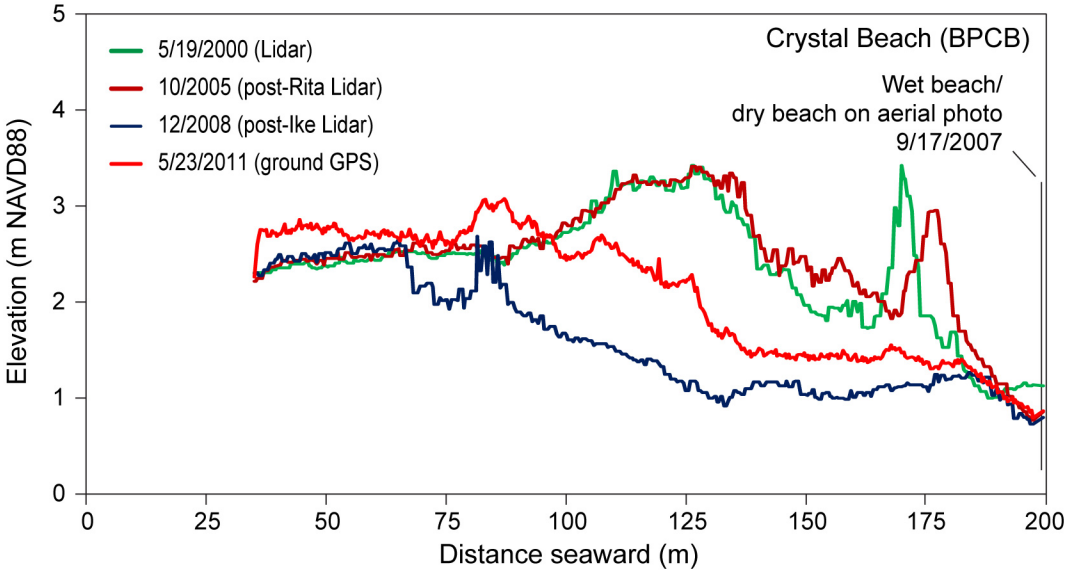

Figure 15. Beach profile on Bolivar Peninsula at Crystal Beach site BPCB (figs. 3, 13) with superimposed wet beach/dry beach boundary mapped on 2007 aerial photographs. Profiles for May 2000, October 2005 (post Rita), and December 2008 (post Ike) were extracted from airborne Lidar surveys. The May 2011 profile was acquired using ground-based differential GPS measurements.

Rates of long-term Gulf shoreline change, calculated from multiple shoreline positions between the 1930s (mid- to late 1800s in some areas) and 2007 (fig. 16), averaged 1.24 m/yr of retreat (table 4) for both net rate and linear regression rate calculations. Updated rates were calculated at 11,731 sites along the entire Texas coast spaced at 50 m. Net retreat occurred at 9,830 (84 percent) and advance occurred at 1,880 (16 percent) over the period of record. The overall rate is lower than the average change rate (retreat at 1.66 m/yr) determined from the most recent previous update (through the mid 1990s to 2000). The previous rates do not include Calhoun, Aransas, Kenedy, and part of Kleberg counties, which are areas of generally low rates of change (slow advance to slow retreat) that, if included, would likely decrease the average net retreat rate for the coast in the earlier calculations. Comparisons of rates in individual counties (table 4) indicate that rates were more erosional in Jefferson, Chambers, Matagorda, and Willacy counties and less erosional in Galveston, Brazoria, Nueces, Kleberg, and Cameron counties. Shorelines along the upper Texas coast (from the mouth of the Colorado River to Sabine Pass) generally retreated at greater rates than those on the central and lower coast. Averages of change rates were retreat at 1.6 m/yr for the upper coast and retreat at 1.0 m/yr for the central and lower coast.

Notable extensive areas of relatively high long-term retreat rates include the High Island to Sabine Pass area, an area on Galveston Island west of the Galveston seawall, the combined deltaic headland of the Brazos and Colorado rivers, Matagorda Peninsula west of the Colorado River, San Jose Island, north Padre Island, and most of the southern half of Padre Island. Areas of general net shoreline advance are found on the upper coast near the Sabine Pass and Bolivar Roads jetties, at the western tip of Galveston Island, on the Brazos/Colorado deltaic headland near the mouth of the Brazos River, toward the western end of Matagorda Peninsula, on the central Texas coast along much of Matagorda Island and near Aransas Pass, and on Padre Island near Baffin Bay and the southern end of the island.

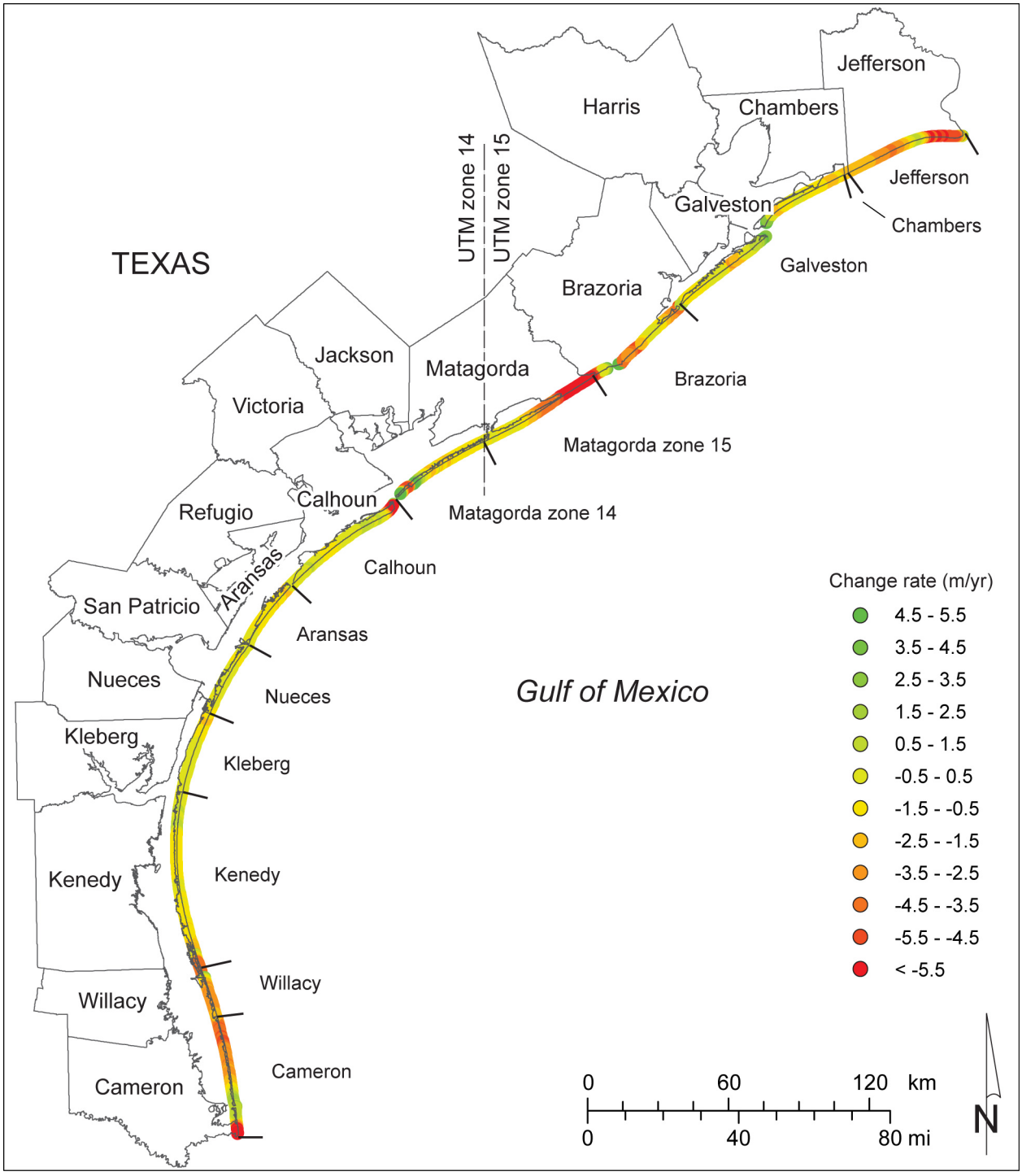

Figure 16. Net rates of long-term change for the Texas Gulf shoreline between Sabine Pass and the Rio Grande calculated from shoreline positions through 2007 (table 3). Change rates at 11,731 individual measurement sites are available on the accompanying data CD in GIS-compatible format.

Table 4. Comparison of historical change rate statistics for the Texas Gulf shoreline calculated for all measurement points along the coast and within individual counties. Net (average) rates and linear regression rates are shown for the 2007 rates. Only linear regression rates were calculated for the 2000 rates. Counties are listed from upper to lower coast (fig. 16).

	Rates through 2007				Rates through 2000	
Area	No.	Net rate (m/yr)	Linear regression rate (m/yr)		No.	Linear regression rate (m/yr)
All counties	11,731	-1.24	-1.24			
Jefferson Co.	1031	-2.80	-2.87		1040	-2.69
Chambers Co.	35	-1.54	-1.63		35	-1.27
Galveston Co.	1756	-0.39	-0.43		1768	-1.15
Brazoria Co.	924	-0.42	-0.22		883	-0.86
Matagorda Co.	1914	-2.10	-2.07		1926	-1.79
Matagorda Co. (zone 15)	1079	-3.55	-3.62		1079	-3.56
Matagorda Co. (zone 14)	854	-0.28	-0.13		847	0.45
Calhoun Co.	1133	-0.83	-0.72		n/a	n/a
Aransas Co.	625	-0.99	-1.13		n/a	n/a
Nueces Co.	667	-0.28	-0.34		669	-0.76
Kleberg Co.	705	-0.54	-0.45		219	-1.11
Kenedy Co.	1522	-0.70	-0.68		n/a	n/a
Willacy Co.	422	-2.63	-2.63		347	-2.39
Cameron Co.	1015	-2.29	-2.39		1017	-2.53

Closely spaced measurement sites allow estimates of land loss to be made. The annual rate of land loss along the Texas Gulf shoreline, updated through 2007, is 73 ha/yr (180 ac/yr). Total Texas Gulf shoreline land loss from a beginning date of 1930 through 2007 is 5,621 ha (13,890 ac).

Upper Texas Coast (Sabine Pass to San Luis Pass)

The upper Texas coast extends from Sabine Pass at the Texas-Louisiana border to San Luis Pass at the southwestern end of Galveston Island (figs. 16, 17), a distance of about 141 km (88 mi). It includes shoreline fronting the Gulf of Mexico within Jefferson, Chambers, and Galveston counties. Major natural geomorphic features and shoreline types are (1) the generally shore-par-

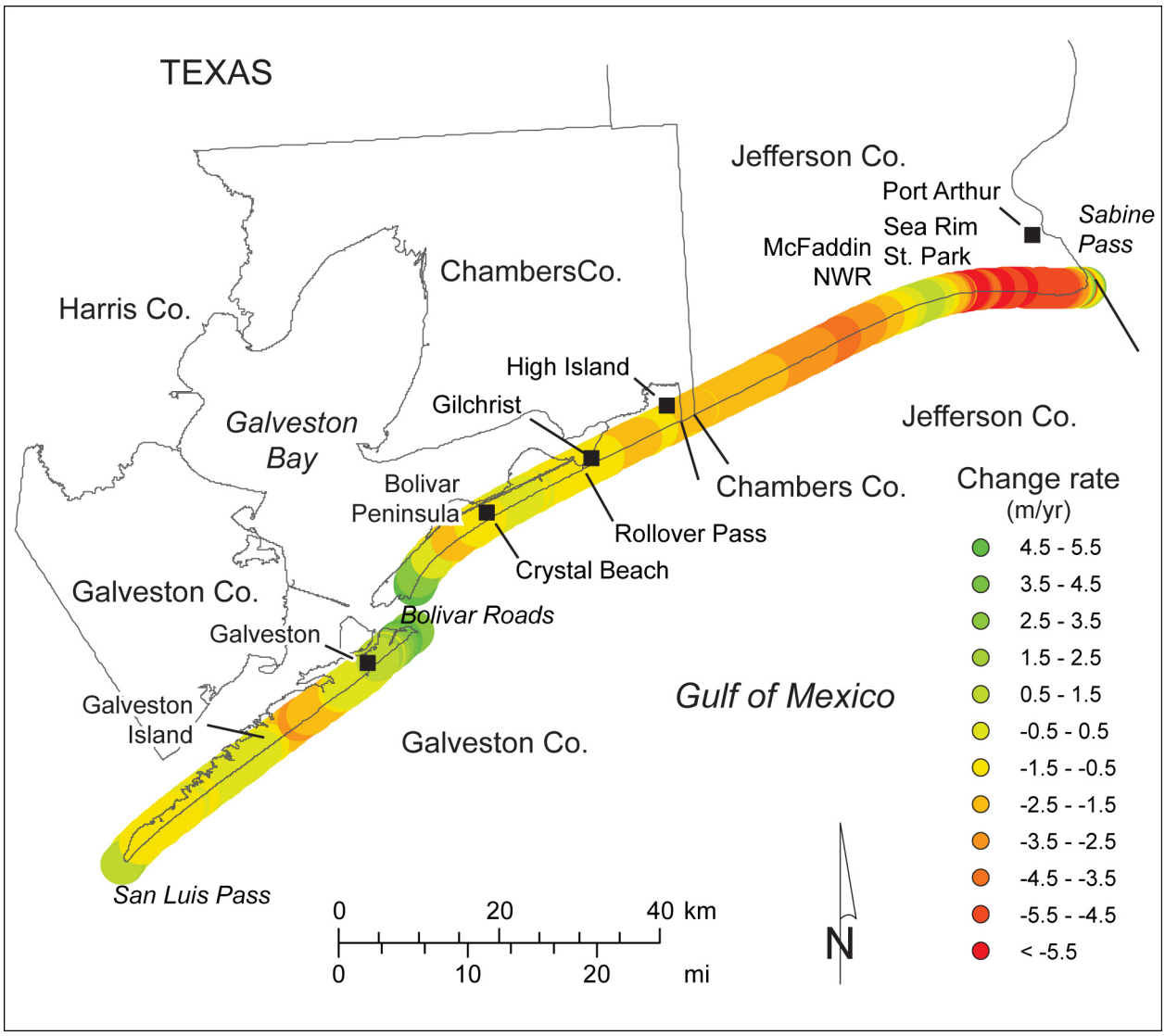

Figure 17. Net rates of long-term change for the upper Texas Gulf shoreline between Sabine Pass and San Luis Pass (Jefferson, Chambers, and Galveston counties) calculated from shoreline positions through 2007 (table 3).

allel beach ridges and intervening swales in the Sabine Pass area, (2) thin, discontinuous sandy beaches that veneer the retreating low, muddy marsh deposits between High Island and Sea Rim State Park, (3) the broad, sandy beach and dune system on Bolivar Peninsula, and (4) the sandy barrier island system at Galveston Island. Major engineered structures that have affected the sediment budget and shoreline change rates include major jetty and dredged channel systems at Sabine Pass and Bolivar Roads, a shallow (1.5 m; 5 ft) dredged channel across Bolivar Peninsula

at Rollover Pass, and the Galveston seawall and groin system on the eastern part of Galveston Island. At Sabine Pass, the south jetty extends about 4 km from the shoreline and protects a channel maintained at a depth of 12 m (40 ft). The Sabine Pass jetties and channel isolate the upper Texas coast from potential easterly sources of longshore sediment. The Bolivar Roads channel, maintained at a depth of 14 m (45 ft), is protected by long jetties that extend 7.6 km (north jetty) and 3.9 km (south jetty) from the shoreline. The jetties and channel serve to compartmentalize the upper Texas coast by blocking longshore transport of sand between Bolivar Peninsula and Galveston Island.

Average net long-term rates of shoreline change for the upper Texas coast counties range from retreat at 0.4 m/yr (Galveston County) to retreat at 2.8 m/yr (Jefferson County, table 4). These rates are similar to those calculated through the mid-1990s to 2000 (average retreat at 1.2 to 2.7 m/yr, table 4). Net rates at individual measuring points range from retreat at 8.5 m/yr to advance at 11.2 m/yr. Land-loss rates averaged 14.4 ha/yr (35.7 ac/yr) in Jefferson County, 0.3 ha/yr (0.7 ac/yr) in Chambers County, and 3.4 ha/yr (8.4 ac/yr) in Galveston County. Net land loss since 1930 is estimated to be 1393 ha (3756 ac) between Sabine Pass and San Luis Pass.

Nearly 88 percent of the measurement sites on the upper Texas coast (2468 of 2810) showed net shoreline retreat through 2007. Long segments of retreating shorelines extend from near Sabine Pass to High Island, between High Island and Gilchrist, on the western part of Bolivar Peninsula southwest of Crystal Beach, on Galveston Island along a 10-km shoreline segment west of the seawall, and on the western end of Galveston Island (fig. 17). Areas of net advance are limited, but include a short shoreline segment adjacent to the south jetty at Sabine Pass, a 3-km-long segment at McFaddin National Wildlife Refuge, shoreline segments a few km long adjacent to the north and south jetties at Bolivar Roads, and the southwestern end of Galveston Island extending 1 to 2 km from San Luis Pass.

Brazos and Colorado Headland (San Luis Pass to Pass Cavallo)

Between San Luis Pass and Pass Cavallo lies the headland of the Brazos and Colorado river deltas and flanking barrier peninsulas Follets Island and Matagorda Peninsula (figs. 16, 18). This segment includes about 143 km (89 mi) of Gulf of Mexico shoreline within Brazoria and Matagorda counties. Major natural geomorphic features are (1) the combined Brazos and Colorado deltaic headland, consisting of semiconsolidated, muddy and sandy sediments deposited by the Brazos and Colorado rivers and overlain by a discontinuous, thin veneer of sandy beach

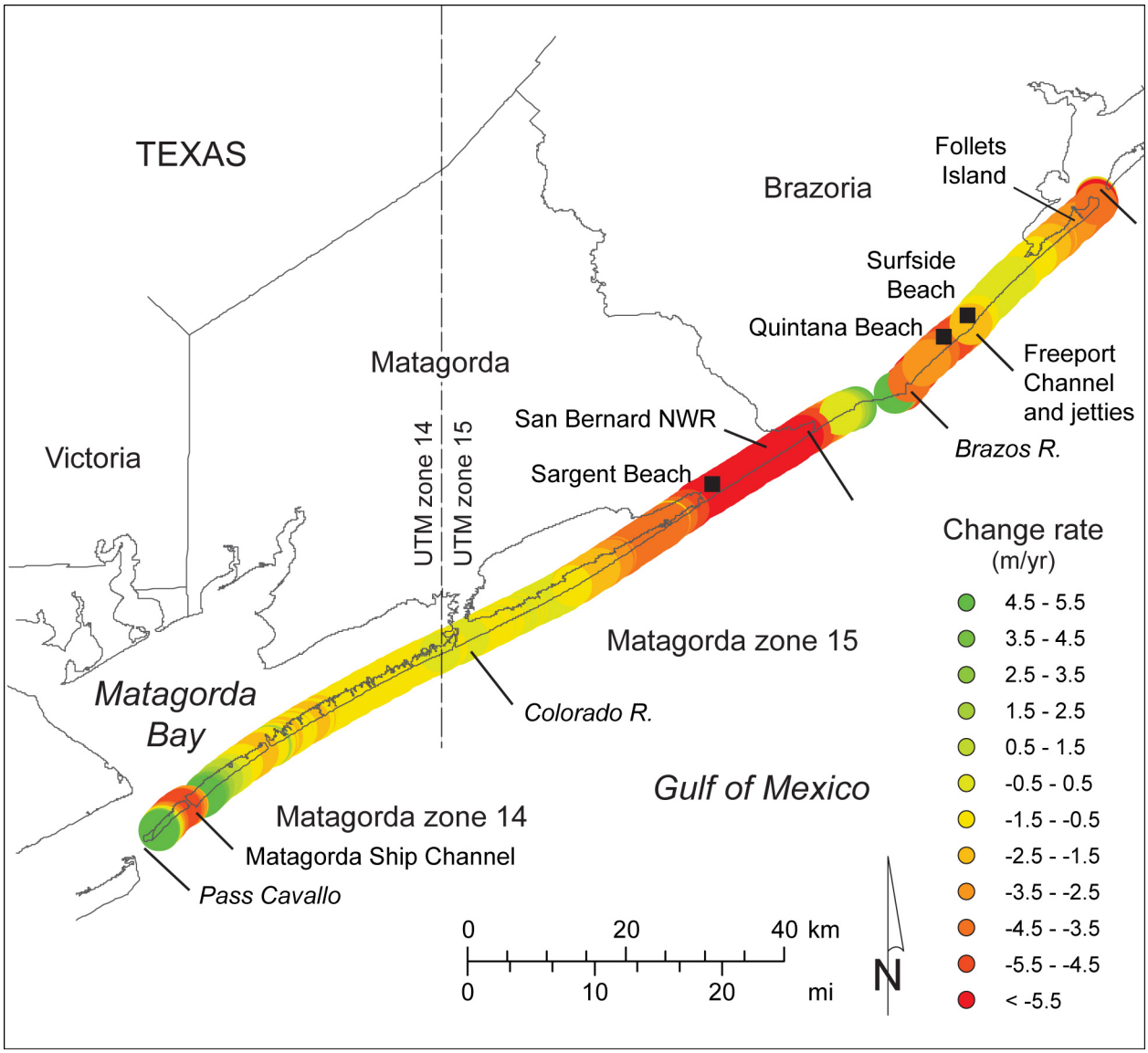

Figure 18. Net rates of long-term change for the Texas Gulf shoreline along the Brazos and Colorado headland between San Luis Pass and Pass Cavallo (Brazoria and Matagorda counties) calculated from shoreline positions through 2007 (table 3).

deposits; (2) a narrow, sandy barrier peninsula extending northeastward from the Brazos headland toward San Luis Pass (including Follets Island); and (3) a narrow, sandy barrier peninsula extending southwestward from the Colorado headland toward Pass Cavallo (Matagorda Peninsula). Sediments eroded by waves at the headland contribute sandy sediments to the flanking barrier peninsulas. In addition, the Brazos and Colorado rivers bring sediment to the coast from their large drainage basins. The drainage basin of the Brazos River covers about 116,000 km^2 in Texas and eastern New Mexico, but its capacity for carrying sediment to the coast during major floods has been reduced by completion of several dams and reservoirs between 1941 and 1969 (Possum Kingdom, Whitney, Granbury, and DeCordova Bend). The drainage basin of the Colorado is nearly as large (103,000 km^2), but its sediment-carrying capacity has also been reduced by nine dams completed in the upper and central basins between 1937 and 1990 (Buchanan, Inks, Tom Miller, Mansfield, Wirtz, Starcke, Thomas, Lee, and Ivie). This segment of Gulf shoreline has been compartmentalized by jetties and dredged channels. Between Quintana and Surfside Beach, the Freeport jetties extend about 1000 m from the shoreline to reduce dredging needs of the Freeport Ship Channel, which has been dredged to a depth of 14 m (45 ft). On Matagorda Peninsula, shorter jetties extend 140 to 240 m seaward from the mouth of the Colorado River. The Matagorda Ship Channel, maintained at a dredged depth of 11 m (36 ft) near the southwestern end of Matagorda Peninsula, is flanked by jetties that extend 880 m (north jetty) and 1600 m (south jetty) into the Gulf.

Net shoreline change rates through 2007 average 0.4 m/yr of retreat in Brazoria County and 2.1 m/yr of retreat in Matagorda County (table 4). This represents a reduction in retreat rate in Brazoria County and an increase in Matagorda County from rates calculated through the mid-1990s to 2000. Net rates of change through 2007 ranged from retreat at 10.2 m/yr to advance at 25.6 m/y. Rates of land loss were 1.9 ha/yr (4.7 ac/yr) for Brazoria County and 20.1 ha/yr (49.7 ac/yr) for Matagorda County. When integrated over the entire measurement period since 1930, estimates of total land loss along the Gulf shoreline are 148 ha (366 ac) in Brazoria County and 1548 ha (3824 ac) in Matagorda County.

There was net shoreline retreat at 2417 of 2837 (85 percent) measurement sites between San Luis Pass and Pass Cavallo. Notable areas of long-term shoreline retreat include Follets Island, the Brazos headland between Surfside Beach and the mouth of the Brazos River and from Sargent Beach to the San Bernard National Wildlife Refuge, and a segment of Matagorda Peninsula southwest of the Matagorda Ship Channel (fig. 18). Shorelines having net advance are limited to short segments on Matagorda Peninsula, including a 3-km-long segment northeast of the mouth of the Colorado River, a 5.5-km-long segment adjacent to the north jetty at the Matagorda Ship Channel, and a 2-km-long segment at the southwestern tip of Matagorda Peninsula.

Central Texas Coast (Pass Cavallo to Packery Channel)

Gulf shorelines along the central Texas coast include those on three sandy barrier islands: Matagorda Island, San Jose Island, and Mustang Island (figs. 16 and 19). These generally sand-rich islands are characterized by broad, sandy beaches and dune systems that reflect the position of the islands within a longshore current convergence zone between the Brazos/Colorado and Rio Grande deltaic headlands. The natural boundaries between these three islands are Cedar Bayou, a tidal inlet between Matagorda and San Jose islands, and Aransas Pass, a tidal inlet between San Jose and Mustang Islands. No rivers reach the Gulf within this segment.

Coastal engineering structures that have compartmentalized the nearshore system are (1) the Matagorda Ship Channel and jetties that restrict sediment transport to Matagorda Island from the northeast, and (2) the jetties at Aransas Pass, which protect the dredged, 14-m (47-ft) deep Corpus Christi Ship Channel. These jetties extend 1100 to 1200 m gulfward from the shoreline, interrupting longshore sand exchange between Mustang and San Jose Islands. Smaller structures with possible local effects include the closed Fish Pass on Mustang Island, where the former dredged channel is filled but short jetties that extend about 150 m from the shoreline remain; and Packery Channel, a newly constructed shallow channel between Mustang and Padre islands that

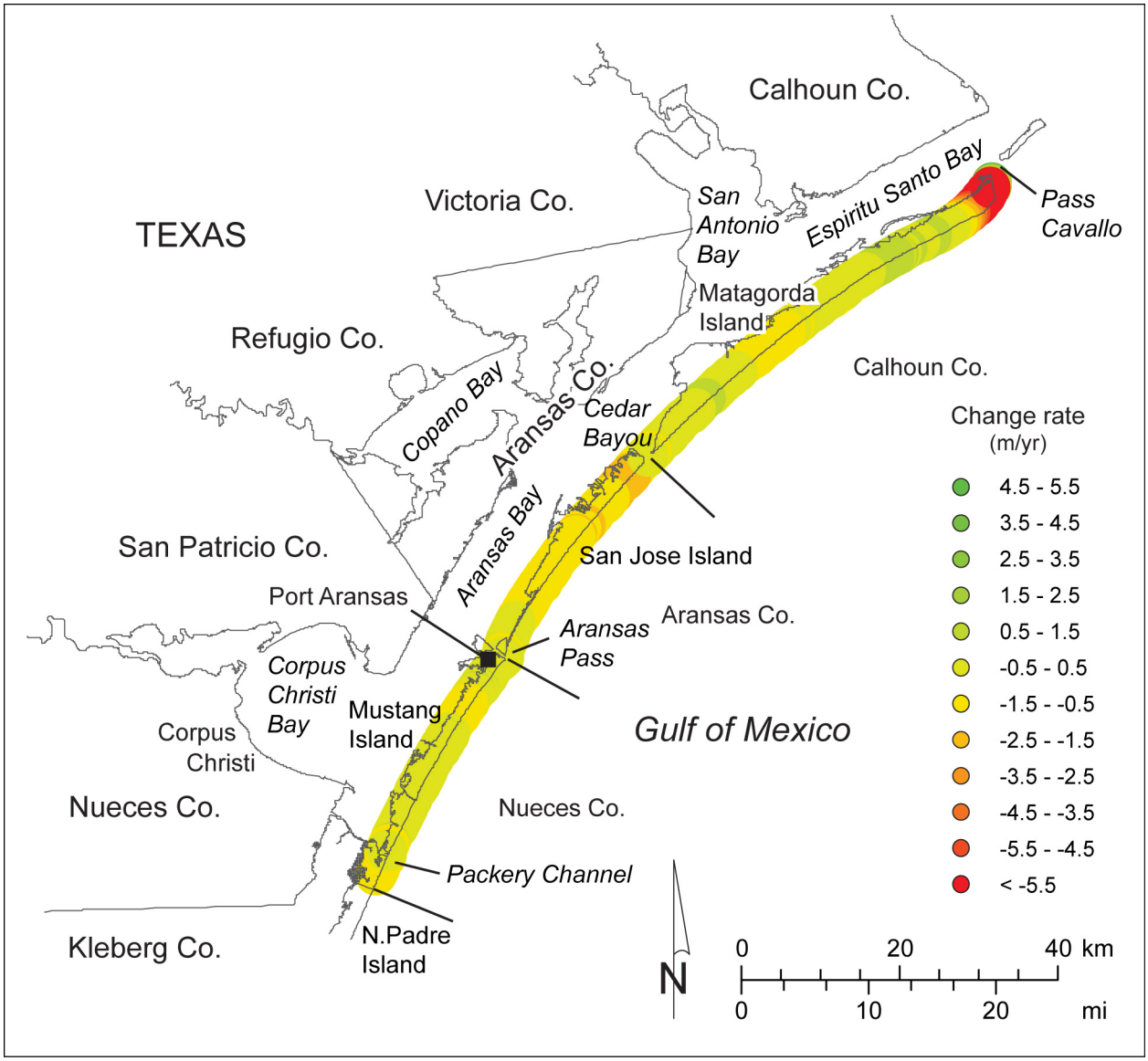

Figure 19. Net rates of long-term change for the central Texas Gulf shoreline between Pass Cavallo and the Packery Channel area (Calhoun, Aransas, and Nueces counties) calculated from shoreline positions through 2007 (table 3).

has been dredged to a nominal depth of 3 m (10 ft) and is protected by jetties that reach 300 m (north jetty) and 365 m (south jetty) beyond the Gulf shoreline.

Long-term Gulf shoreline change rates within this segment of the Texas coast were calculated at 2,419 sites over a distance of 121 km (75 mi) between Pass Cavallo and the southern end of Mustang Island (table 4; fig. 19). Net shoreline change rates calculated through 2007 averaged retreat at 0.83 m/yr for Matagorda Island (Calhoun County), retreat at 0.99 m/yr for San Jose

Island (Aransas County), and retreat at 0.28 m/yr for Mustang Island (Nueces County). Annual rates of land loss estimated from these updated rates are 4.7 ha/yr (11.6 ac/yr) on Matagorda Island, 3.1 ha/yr (7.6 ac/yr) on San Jose Island, and 1.0 ha/yr (2.3 ac/yr) on Mustang Island. Estimated total land loss along the Gulf shoreline since 1930 is 362 ha (894 ac) on Matagorda Island, 237 ha (586 ac) on San Jose Island, and 73 ha (181 ac) on Mustang Island.

The majority of measuring sites underwent net shoreline retreat (1872 of 2419; 77 percent). Net rates at individual sites ranged from retreat at 17 m/yr to advance at 18 m/yr. Nearly half the Gulf shoreline of Matagorda Island has advanced since 1937, albeit at low rates except along a short segment where the island has migrated toward Pass Cavallo at its northeastern end. Sites along short shoreline segments (1.4 to 3.3 km long) near the north and south jetties of the Corpus Christi Ship Channel recorded minor net shoreline advance. Highest rates of net retreat (more than 3 m/yr) were measured along a 6-km-long segment of Matagorda Island near Pass Cavallo. Net retreat rates greater than 1 m/yr were measured along all of San Jose Island except the southern 7 km of the island, along a 5-km-long segment in the middle part of Mustang Island, and along the southern tip of Mustang Island. Net retreat rates elsewhere were less than 1 m/yr.

Lower Coast (Padre Island)

The lower coast segment encompasses 183 km (114 mi) of Gulf shoreline within Kleberg, Kenedy, Willacy, and Cameron counties (figs. 16, 20), where shoreline change rates were calculated at 3,663 sites. The principal natural geomorphic feature in this area is Padre Island, a long Holocene barrier island that broadens from a narrow peninsula at Brazos Santiago Pass to a broad, sandy barrier island having a well-developed dune system throughout most of its length. The Rio Grande enters the Gulf of Mexico within this segment and has created a large fluvial/deltaic headland that forms the southern boundary of a regional longshore current cell that is bounded on the north by the Brazos/Colorado headland. The Rio Grande has a large drainage basin (471,900 km^2) that extends into Mexico, New Mexico, and Colorado, but dams constructed on the middle and lower parts of the basin in 1954 (Falcon) and 1969 (Amistad), combined with

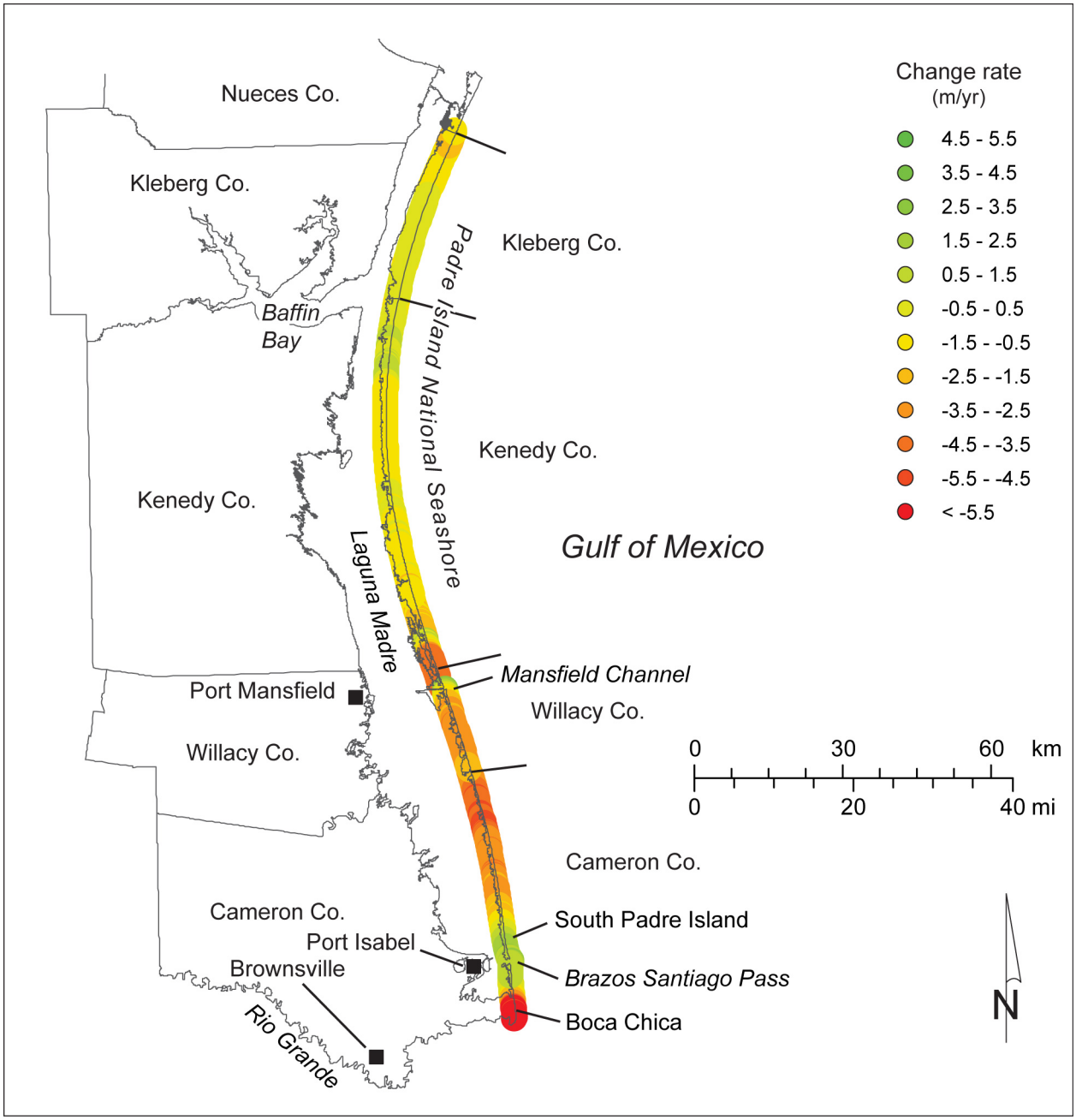

Figure 20. Net rates of long-term change for the lower Texas Gulf shoreline along Padre Island (Kleberg, Kenedy, Willacy, and Cameron counties) calculated from shoreline positions through 2007 (table 3).

extensive irrigation use of Rio Grande water on the coastal plain, has reduced the sediment delivered to the coast.

Most of Padre Island is undeveloped, except for intensive development at its northern extremity and at the southern tip of the island (the city of South Padre Island). Engineering structures that have affected shoreline position include (1) the jetties and associated ship channel at Brazos Santiago Pass, where the 13-m (44-ft) deep channel is flanked by jetties that reach 870 m (north jetty) and 490 m (south jetty) into the Gulf; and (2) the shallower Port Mansfield Channel and its 620-m (north) and 140-m (south) jetties that protect the 5-m (15-ft) deep channel.

Net shoreline change rates updated through 2007 range from average retreat at 0.54 m/yr in Kleberg County to average retreat at 2.63 m/yr in Willacy County (fig. 20, table 4). Average retreat rates through 2007 are slightly higher for Willacy County than they were through 2000, whereas average retreat rates in Cameron County through 2007 were slightly lower than previous rates (table 4). Rates of land loss through 2007 are 1.9 ha/yr (4.7 ac/yr) for Kleberg County, 5.4 ha/yr (13.2 ac/yr) for Kenedy County, 5.6 ha/yr (13.7 ac/yr) for Willacy County, and 11.6 ha/yr (28.7 ac/yr) for Cameron County. Estimated cumulative land loss for these counties since 1930 is 147 ha (363 ac) for Kleberg County, 413 ha (1020 ac) for Kenedy County, 428 ha (1057 ac) for Willacy County, and 893 ha (2207 ac) for Cameron County.

Despite the location of much of Padre Island in a longshore drift convergent zone, net shoreline retreat was found at 3073 of 3663 measurement sites (84 percent). Net change rates at individual sites ranged from advance at 3.2 m/yr to retreat at 7.5 m/yr. Net advancing shorelines include two nearly 5-km-long segments adjacent to the north and south jetties at Brazos Santiago Pass, a 15-km-long segment in the Little Shell Beach area on Padre Island National Seashore near Baffin Bay, and a 5-km-long segment on the northern part of Padre Island National Seashore in central Kleberg County. Highest rates of net retreat (greater than 3 m/yr) were measured along a 8-km-long segment north of the Mansfield Channel jetties, along a 23-km-long segment in northern Cameron County (fig. 20), and along a 3-km-long segment south of Brazos Santiago Pass

at Boca Chica. Lower net retreat rates were measured along most of Padre Island in Kleberg, Kenedy, Willacy, and Cameron counties.

CONCLUSIONS

Long-term rates of Texas Gulf shoreline change have been updated through 2007 from a series of shoreline positions that include those from 1800s topographic charts (in selected areas), aerial photography from the 1930s through 2007, ground GPS surveys from the mid-1990s, and an airborne Lidar survey conducted in 2000.

From 1993 to 2007, the period that would most influence changes in rates between this update and the previous one (through the mid-1990s to 2000), tropical cyclone frequency was near the historical incidence of 0.8 cyclones per year. There were nine tropical storms and four hurricanes that made landfall on the Texas coast, including five on the upper coast, five on the central coast, and three on the lower coast. Relative sea-level rise rates at Galveston for the period were at the low end of historically observed rates (2.1 to 3.7 mm/yr) and were near global (eustatic) rates.

Change rates calculated at 11,731 sites spaced at 50-m intervals averaged net retreat at 1.24 m/yr through 2007. Average change rates were more recessional on the upper Texas coast (-1.6 m/yr) than they were on the central and lower coast (-1.0 m/yr). Annual rates of land loss along the Texas Gulf shoreline average 73 ha/yr (180 ac/yr). Total estimated land loss since 1930, when aerial photography-based shoreline monitoring became possible, is estimated to be 5,620 ha (13,890 ac).

Aerial photography flown in 2007 was chosen to update shoreline change rates because it was the latest coast-wide imagery available that preceded landfall of Hurricane Ike (2008). Ike caused significant shoreline change on the upper Texas coast. The next update is expected to use shoreline position extracted from an upcoming airborne Lidar survey of the Texas Gulf shoreline in spring 2012, a date that allows nearly four years of post-Ike beach recovery.

ACKNOWLEDGMENTS

This project was supported by grant no. 10-041-000-3737 from the General Land Office of Texas to the Bureau of Economic Geology, The University of Texas at Austin. Jeffrey G. Paine served as the principal investigator. The project was funded under a Coastal Management Program (Cycle 14) grant made available to the State of Texas by the U.S. Department of Commerce, National Oceanic and Atmospheric Administration pursuant to the Federal Coastal Zone Management Act of 1972. Additional funds from the State of Texas were provided through the Coastal Erosion Planning and Response Act (CEPRA) program administered by the General Land Office. Ray Newby and Melissa Porter (General Land Office) served as project managers.

REFERENCES

Anders, F. J., and Byrnes, M. R., 1991: Accuracy of shoreline change rates as determined from maps and aerial photographs: Shore and Beach, v. 59, p. 17-26.

Barnett, T. P., 1983, Global sea level: estimating and explaining apparent changes: in Magoon, O. T., and Converse, H., editors, Coastal Zone ‘83, Proceedings of the Third Symposium on Coastal and Ocean Management, v. 3, p. 2777-2783.

Bruun, P., 1954, Coastal erosion and development of beach profiles: Technical Memorandum, v. 44, Beach Erosion Board, U. S. Army Corps of Engineers, 82 p.

Bruun, P., 1962, Sea-level rise as a cause of shore erosion: Proceedings, American Society of Civil Engineers, Journal of the Waterways and Harbors Division, v. 88, p. 117-130.

Bruun, P., 1988, The Bruun rule of erosion by sea-level rise: a discussion of large-scale two- and three-dimensional usages: Journal of Coastal Research, v. 4, p. 627-648.

Cazenave, A., and Nerem, R. S., 2004, Present-day sea level change: observations and causes: Reviews of Geophysics, v, 42, RG3001, doi: 1029/2003RG000139, 20 p.

Church, J. A., and White, N. J., 2006, A 20th century acceleration in global sea-level rise: Geophysical Research Letters, v. 33: L01602, doi: 10.1029/2005GL024826.

Cooper, J. A. G., and Pilkey, O. H., 2004, Sea-level rise and shoreline retreat: time to abandon the Bruun Rule: Global and Planetary Change, v. 43, p. 157-171.

Crowell, M., Leatherman, S. P., and Buckley, M. K., 1991, Historical shoreline change: error analysis and mapping accuracy: Journal of Coastal Research, v. 7, no. 3, p. 839-852.

Emery, K. O., 1980, Relative sea levels from tide-gauge records: Proceedings, National Academy of Sciences, USA, v. 77: p. 6968-6972.

FitzGerald, D. M., Fenster, M. S., Argow, B. A., and Buynevich, I. V., 2008, Coastal impacts due to sea-Level rise: Annual Review of Earth and Planetary Sciences, v. 36, p. 601-647.

Gibeaut, J. C., Hepner, Tiffany, Waldinger, Rachel, Andrews, John, Gutierrez, Roberto, Tremblay, T. A., and Smyth, Rebecca, 2001, Changes in Gulf shoreline position, Mustang and North Padre Islands, Texas: Bureau of Economic Geology, The University of Texas at Austin, Report to the Texas Coastal Coordination Council and the General Land Office, contract no. 00-002r, 29 p.

Gibeaut, J. C., White, W. A., Hepner, Tiffany, Gutierrez, Roberto, Tremblay, T. A., Smyth, R. A., and Andrews, John, 2000, Texas Shoreline Change Project: Gulf of Mexico shoreline change from the Brazos River to Pass Cavallo: Bureau of Economic Geology, The University of Texas at Austin, Report to the Texas Coastal Coordination Council and the General Land Office, contract no. NA870Z0251, 32 p.

Gornitz, V., Lebedeff, S., and Hansen, J., 1982, Global sea level trend in the past century: Science, v. 215, p. 1611-1614.

Gornitz, V., and Lebedeff, S., 1987, Global sea-level changes during the past century: in Nummedal, D., Pilkey, O. H., and Howard, J. D., editors, Sea level fluctuation and coastal evolution: Society of Economic Paleontologists and Mineralogists Special Publication 41, p. 3-16.

Gutenberg, B., 1941, Changes in sea level, postglacial uplift, and mobility of the Earth's interior: Geological Society of America Bulletin, v. 52, p. 721-772.

Hayes, M. O., 1967, Hurricanes as geological agents: case studies of hurricanes Carla, 1961, and Cindy, 1963: The University of Texas at Austin, Bureau of Economic Geology Report of Investigations No. 61, 54 p.

Leuliette, E. W., and Miller, L., 2009, Closing the sea level rise budget with altimetry, Argo, and GRACE: Geophysical Research Letters, v. 36, L04608, doi:10.1029/2008GL036010.

Lyles, S. D., Hickman, L. E., Jr., and Debaugh, H. A., Jr., 1988, Sea level variations for the United States, 1855-1986: National Ocean Service, Rockville, Maryland, 182 p.

Moore, L. J., 2000, Shoreline mapping techniques: Journal of Coastal Research, v. 16, no. 1, p. 111-124.

Morton, R. A., 1974, Shoreline changes on Galveston Island (Bolivar Roads to San Luis Pass), an analysis of historical changes of the Texas Gulf Shoreline: The University of Texas at Austin, Bureau of Economic Geology Geological Circular 74-2, 34 p.

Morton, R. A., 1975, Shoreline changes between Sabine Pass and Bolivar Roads: The University of Texas at Austin, Bureau of Economic Geology Geological Circular 75-6, 43 p.

Morton, R. A., 1977, Historical shoreline changes and their causes, Texas Gulf Coast: Gulf Coast Association of Geological Societies Transactions, v. 27, p. 352–364. Reprinted as Bureau of Economic Geology Geological Circular 77-6, 13 p.

Morton, R. A., 1997, Gulf shoreline movement between Sabine Pass and the Brazos River, Texas: 1974 to 1996: Bureau of Economic Geology Geological Circular 97-3, 46 p.

Morton, R. A., Leach, M. P., and Cardoza, M. A., 1993, Monitoring beach changes using GPS surveying techniques: Journal of Coastal Research, v. 9, p. 702-720.

Morton, R. A., Miller, T. L., and Moore, L. J., 2004, National assessment of shoreline change, part 1: historical shoreline changes and associated coastal land loss along the U.S. Gulf of Mexico: U.S. Geological Survey Open-File Report 2004-1043, 42 p.

Morton, R. A., and Paine, J. G., 1985, Beach and vegetation-line changes at Galveston Island, Texas: erosion, deposition, and recovery from Hurricane Alicia: The University of Texas at Austin, Bureau of Economic Geology Geological Circular 85-5, 39 p.

Morton, R. A., and Paine, J. G., 1990, Coastal land loss in Texas: an overview: Transactions, Gulf Coast Association of Geological Societies, v. 40, p. 625-634.

Morton, R. A., Paine, J. G., and Gibeaut, J. C., 1994, Stages and durations of post-storm beach recovery, southeastern Texas coast, U.S.A.: Journal of Coastal Research, v. 10, p. 884–908.

Morton, R. A., and Pieper, M. J., 1975a, Shoreline changes on Brazos Island and South Padre Island (Mansfield Channel to mouth of the Rio Grande), an analysis of historical changes of the Texas Gulf shoreline: The University of Texas at Austin, Bureau of Economic Geology, Geological Circular 75-2, 39 p.

Morton, R. A., and Pieper, M. J., 1975b, Shoreline changes in the vicinity of the Brazos River delta (San Luis Pass to Brown Cedar Cut): The University of Texas at Austin, Bureau of Economic Geology Geological Circular 75-4, 47 p.

Morton, R. A., and Pieper, M. J., 1976, Shoreline changes on Matagorda Island and San Jose Island (Pass Cavallo to Aransas Pass): The University of Texas at Austin, Bureau of Economic Geology Geological Circular 76-4, 42 p.

Morton, R. A., and Pieper, M. J., 1977a, Shoreline changes on Mustang Island and North Padre Island (Aransas Pass to Yarborough Pass): The University of Texas at Austin, Bureau of Economic Geology Geological Circular 77-1, 45 p.

Morton, R. A., and Pieper, M. J., 1977b, Shoreline changes on central Padre Island (Yarborough Pass to Mansfield Channel): The University of Texas at Austin, Bureau of Economic Geology Geological Circular 77-2, 35 p.

Morton, R. A., Pieper, M. J., and McGowen, J. H., 1976, Shoreline changes on Matagorda Peninsula (Brown Cedar Cut to Pass Cavallo): The University of Texas at Austin, Bureau of Economic Geology Geological Circular 76-6, 37 p.

Paine, J. G., 1991, Late Quaternary depositional units, sea level, and vertical movement along the central Texas coast: Ph. D. dissertation, University of Texas at Austin, Austin, Texas, 256 p.

Paine, J. G., 1993, Subsidence of the Texas coast: inferences from historical and late Pleistocene sea levels: Tectonophysics, v. 222, p. 445–458.

Paine, J. G., and Morton, R. A., 1989, Shoreline and vegetation-line movement, Texas Gulf Coast, 1974 to 1982: The University of Texas at Austin, Bureau of Economic Geology Geological Circular 89-1, 50 p.

Peltier, W. R., and Tushingham, A. M., 1989, Global sea level rise and the greenhouse effect: might they be connected?: Science, v. 44, p. 806-810.

Penland, S., and Ramsey, K., 1990, Sea-level rise in Louisiana and the Gulf of Mexico: 1908-1988: Journal of Coastal Research, v. 6, no. 2, p. 323-342.

Price, W. A., 1956, Hurricanes affecting the coast of Texas from Galveston to the Rio Grande: U.S. Army Corps of Engineers Beach Erosion Board, Technical Memorandum No. 78, 35 p.

Roth, David, 2010, Texas hurricane history: National Weather Service, Camp Springs, Marlyand, 83 p. http://origin.hpc.ncep.noaa.gov/research/txhur.pdf

Shalowitz, A. L., 1964, Shore and beach boundaries: U.S. Department of Commerce, Publication 10-1, 749 p.

Simpson, R. H., and Riehl, H., 1981, The hurricane and its impact: Baton Rouge, Louisiana State University Press, 398 p.

Swanson, R. L., and Thurlow, C. I, 1973, Recent subsidence rates along the Texas and Louisiana coast as determined from tide measurements: Journal of Geophysical Research, v. 78, p. 2665-2671.

Thieler, E. R., Himmelstoss, E. A., Zichichi, J. L., and Ergul, Ayhan, 2009, Digital Shoreline Analysis System (DSAS) version 4.0 — An ArcGIS extension for calculating shoreline change: U.S. Geological Survey Open-File Report 2008-1278.